

## N O T I C E

THIS DOCUMENT HAS BEEN REPRODUCED FROM  
MICROFICHE. ALTHOUGH IT IS RECOGNIZED THAT  
CERTAIN PORTIONS ARE ILLEGIBLE, IT IS BEING RELEASED  
IN THE INTEREST OF MAKING AVAILABLE AS MUCH  
INFORMATION AS POSSIBLE

## N O T I C E

THIS DOCUMENT HAS BEEN REPRODUCED FROM  
MICROFICHE. ALTHOUGH IT IS RECOGNIZED THAT  
CERTAIN PORTIONS ARE ILLEGIBLE, IT IS BEING RELEASED  
IN THE INTEREST OF MAKING AVAILABLE AS MUCH  
INFORMATION AS POSSIBLE

NASA TECHNICAL MEMORANDUM

NASA TM-75747

CHARACTERIZATION AND GROWTH OF EPITAXIAL LAYERS  
OF GaAs EXHIBITING HIGH RESISTIVITY FOR IONIC IMPLANTATION

Translation of "Croissance et Caracterisation des couches epitaxiales de GaAs de haute resistivite pour implantation ionique", Laboratories d'Electronique et de Physique Appliquee, DGRST, Limeil-Brevannes, France, Final Report, Dec. 1977, LEP-79/19. SME-441-H, and DGRST 76-7-0067, pp 1-90

(NASA-TM-75747) CHARACTERIZATION AND GROWTH  
OF EPITAXIAL LAYERS OF GS EXHIBITING HIGH  
RESISTIVITY FOR IONIC IMPLANTATION (National  
Aeronautics and Space Administration) 91 p  
HC A05/MF A01

N80-27197

Unclassified  
CSCL 20L G3/76 23599



NATIONAL AERONAUTICS AND SPACE ADMINISTRATION  
WASHINGTON, D. C. 20546 DECEMBER 1979

## STANDARD TITLE PAGE

1. Report No. NASA TM-75747	2. Government Accession No.	3. Recipient's Catalog No.	
4. Title and Subtitle CHARACTERIZATION AND GROWTH OF EPITAXIAL LAYERS OF GaAs EXHIBITING HIGH RESISTIVITY FOR IONIC IMPLANTATION		5. Report Date December 1979	
7. Author(s)		6. Performing Organization Code	
9. Performing Organization Name and Address SCITRAN Box 5456 Santa Barbara, CA 93108		8. Performing Organization Report No.	
12. Sponsoring Agency Name and Address National Aeronautics and Space Administration Washington, D. C. 20546		10. Work Unit No.	
13. Type of Report and Period Covered Translation		11. Contract or Grant No. NASW-3198	
15. Supplementary Notes Translation of "Croissance et Caracterisation des couches epitaxiales de gaAs de haute resistivite pour implantation ionique," Laboratories d'Electronique et de Physique Appliquee, DGRST, Limeil-Brevannes, France, Final Report, Dec. 1977, LEP-79/19. SME-441-H, and DGRST 76-7-0067, pp 1-90 (N79-24881)		14. Sponsoring Agency Code	
16. Abstract  This study shows that, by either classical or low-temperature epitaxial growth techniques, it is possible to control the deposition of buffer layers of GaAs on semi-insulating substrates and to obtain the resistivity and purity desired.			
17. Key Words (Selected by Author(s))		18. Distribution Statement  Unclassified - Unlimited	
19. Security Classif. (of this report) Unclassified	20. Security Classif. (of this page) Unclassified	21. No. of Pages 91	22.

TABLE OF CONTENTS

	<u>Page</u>
INTRODUCTION	1
I - CONDUCT OF THE RESEARCH	3
1 - Method of Growth	4
1. Classical method	4
2. Low temperature method	5
2 - Definition of the dead layer	6
3 - Characterization Techniques	6
1. Hall Effect	7
2. Photo Hall	8
3. Trap spectroscopy by current transients with optical excitation	10
4. Cathodoluminescence	12
II- ANALYSIS AND INTERPRETATION	13
1 - Characterization of $n^-$ levels	13
1. Measurement of $\mu$ and $n^-$	13
2. Luminescence of acceptor centers	16
3. Diffusion model	18
2 - Characterization of the dead layers	19
1. Deposits obtained by the classical method	19
A - Mobilities during illumination	19
B - Identification of deep traps	20
C - Compensation by shallow acceptors	23
2. Depots obtained by low temperatures growing ( $650^\circ\text{C}$ ) with a source of GaAs doped with Cr.	24
3. Relative thickness of the $n^-$ and dead layers	26
III-IMPLANTATION	28

CONCLUSIONS

REFERENCES

FIGURE CAPTIONS

APPENDIX I: Differential calculation of mobilities and doping levels in Hall effect.

APPENDIX II: Article submitted for publication in Applied Physics Letters: "Deep Level Spectroscopy in High Resistivity Material," C. Hurtés, M. Boulou, M. Mitonneau, D. Bois.

### ANNOTATION

This study shows that, by either classical or low-temperature epitaxial growth techniques, it is possible to control the deposition of buffer layers of GaAs on semi-insulating substrates and to obtain the resistivity and purity desired.

Original methods of characterization, such as photohall effect and spectroscopy of shallow or deep levels as a function of depth, reveal two regions in these layers: one very pure and of high mobility, the other, called the "dead layer", closer to the substrate, which is highly resistive and strongly compensated. This compensation was attributed to diffusion of shallow acceptors (C,Cu) and of deep centers (Cr or Fe) from the interface.

Implantations of  $\text{Se}^+$  in these layers has led to the realization of PET devices the performance of which shows a marked improvement with respect to direct implantation into the substrate.

## INTRODUCTION

The interest of GaAs for integrated circuits has been confirmed since this study was first proposed. At the same time it/4\* has become apparent that the progress toward device realization has begun to be increasingly limited by the materials. While the classical epitaxial layers (about  $0.2 \mu\text{m}$  thick,  $n = 10^{17} \text{ atom/cm}^3$ ) are well suited for technological studies [1] and for first realizations [2], [3], in SSI or MSI, the more interesting extension to LSI requires the use of "normally-off" transistors, which require very thin active layers ( $\leq 0.1 \mu\text{m}$ ). It seems today however that the best method-if not the only possible one-for obtaining these layers would be ion implantation.

For ion implantation, progress seems to be particularly limited by the substrates. A significant effort has already been made at RTC to improve the quality and the homogeneity of crystals obtained by the Bridgman method. Nevertheless, this material remains still insufficiently known and controllable, which does not permit today a reproducibility sufficient for circuits of high density of integration. In addition, the same problems exist for foreign manufacturers; only one Japanese supplier (Sumitomo) seems to have found a good compromise for the substrates intended for implantation. Some actions have been undertaken or are envisaged to ameliorate this situation-notably by the utilization of Czochralsky pulling but success does not yet seem to be at hand.

It is in this context that we have written our study "Growth and characterization of epitaxial layers of GaAs of high resistivity for ion implantation", that is, the study of epitaxial "buffer" layers of several microns, purer and more easily controllable than semi-insulating substrates, and in which the implantation can therefore be carried out under the best conditions.

---

\*Numbers in margins indicate foreign pagination

The general objective was to understand the properties of this layer, partly by means of diagnostic characterizations and partly by establishing a correlation between the crystal properties and the conditions of growth. Afterwards, layers of high resistivity of the best quality should be tested in ion implantation.

## I - CONDUCT OF THE RESEARCH

/6

The progress of the work conformed to the proposed plan. We will present this progress in terms of the two large axes of the research: growth and characterization.

The following participated in this study:

Michel Boulou	(Cathodoluminescence)
Jean-Marie Durand	(Low-temperature epitaxy)
Jean Hallais	(Coordination with implantation)
Laszlo Hollan	(Growth)
Chantal Hurtet	(Ensemble of characterization)
Genevieve Mannechez	(Technical assistant for growth)

Spectroscopic measurements of traps (OTCS) were carried out on the DLTS equipment and with the aid of MM. Mitonneau and G. M. Martin, implantations were carried out by MM. Favennec and Pelous (CNET), the annealing of implanted samples by M. Venger, and the field-effect transistors by the team of D. Boccon-Gibod.

In order to present the problems as completely as possible, we have been led to include in this report certain results obtained prior to the contractual period.

## I - 1. Method of Growth

/7

Two methods were utilized for the growth of high resistivity epitaxial layers.

### I - 1.1. Classical Method AsCl<sub>3</sub>/Ga/H<sub>2</sub> [4]

The principle consists of transporting gallium by arsenic trichloride in a current of hydrogen.

The deposition temperature  $T_D$  is normally in the neighborhood of 750°C. It is possible to lower it to 700°C [5] and even below [6]. However, below 700°C the operating conditions become very critical and the results quite unrepeatable. Most of the studies were carried out between 750 and 770°C, with several growths at 720°C.

In addition, the use of argon as a vector gas instead of hydrogen has permitted the growth temperature to be lowered to 650°C, so that the influence of  $T_D$  can be studied over a very extended range of values.

In this method, DiLorenzo [7] showed that the residual doping is due principally to silicon. This can be reduced by increasing the partial pressure of HCl, by means of that of AsCl<sub>3</sub>. The mole fraction of AsCl<sub>3</sub> ( $MF = P_0 \cdot d$ ), equal to the partial pressure of AsCl<sub>3</sub> multiplied by the dilution is a second important parameter. The use of this method [8], which has an interesting variant developed by Nozaki [9] has led to our obtaining epitaxial layers of which the residual doping is on the order of  $n \approx 10^{14}$  at  $\text{cm}^{-3}$  and which presents elevated mobilities at low temperatures ( $\mu_{77 \text{ K}} = 90$  to 150,000  $\text{cm}^2 \text{V}^{-1} \text{s}^{-1}$ ).

However, certain aspects related to this technique of growth have not thus far been the object of special study. Thus problems

such as the reproducibility at high MF, the influence of the substrate, of the duration and the temperature of growth have been studied in the course of this contract by means of a significant number of tests.

### I - 1.2. Low-temperature method $\text{AsCl}_3/\text{GaAs}/\text{H}_2$

This "low-temperature" method [6] is based on the transport of solid GaAs by  $\text{AsCl}_3$  in a hydrogen current. It was developed in our laboratory. The deposition temperature  $T_D$  is around  $630^\circ\text{C}$ .

If the solid polycrystalline material used as a source of GaAs is conveniently doped with Cr, the epitaxial deposit has an elevated resistance. This is obtained not by reducing the residual doping n as in the classic method, but by compensation of this residual doping. The intrinsic purity of these epitaxial layers is thus a priori low. Practically, in this case, the carrier mobility at low temperature ( $77^\circ\text{K}$ ) does not exceed  $30,000 \text{ cm}^2\text{V}^{-1}\text{s}^{-1}$ .

On the other hand, this method is better adapted to industrial development. Its utilization is easier, and it allows one to overcome problems related to the saturation of Ga (instability of the crust of GaAs formed).

Furthermore, lowering the source and deposition temperatures diminishes contamination by silicon [7] and limits the influence of the substrate.

Finally, its utilization has led to good results in terms of devices [6].

Before evaluating, for implantation, the interest of these layers which generally present a high resistivity, we should define what is mean by a "dead layer."

## I - 2. Definition of the dead layer

/9

The first result of this research was the definition of two types of buffer layers (which may or may not be present simultaneously), the "dead layer" and the  $n^-$  layer. This observation has since been confirmed by DiLorenzo [5].

- Epitaxial layers of high purity and on which one measures elevated mobilities at low temperature are called  $n^-$  layers (with  $n < 10^{15}$ ). The ambient resistivity of these layers in general does not exceed 10  $\Omega\text{cm}$ .
- Epitaxial layers of a priori unknown purity, presenting a high resistivity ( $p > 10^3 \Omega\text{cm}$ ) are called "dead layers".

This high resistivity is explained by strong compensation in the layer, intentional or accidental, due to either the growth or the substrate.

It was thus necessary to understand better the nature of the "dead layer" and we have had recourse to several means of characterization.

## I - 3. Characterization techniques

/10

The most important parameters to study in these buffer layers are the mobility and the doping level, which justified intensive use of Hall effect measurements.

However, for interfacial zones of very high resistivity, classical electrical measurements were not usable, and we had to develop other original methods, which included the photo-Hall effect and spectroscopy of traps using optical excitation.

Complementary analyses of cathodoluminescence were also carried out.

These different techniques have permitted us to carry out:

- measures of mobility and doping
- analysis of deep traps  
shallow traps present in the material.

At the same time, the evolution of electrical parameters and the presence of shallow or deep impurity levels were followed as a function of depth in the epitaxial layer.

### I - 3.1. Hall Effect

The classical technique of Van derPauw [10] was used.

Samples cut into clover shapes were subjected to successive etches in a solution of  $H_2SO_4/H_2O_2/H_2O$  (5/1/1), the etched thicknesses being carefully controlled. The measurement was automated. A magnetic field of 3kG was used, and the sample was placed into the dark.

Profiles of mobility and doping in the  $n^-$  layers were thus obtained at 300°K and at 77°K (figure 1).

It should be noted that the Hall measurement represents an /11 average over the entire thickness of the epitaxial layer (including the very resistive part).

A differential calculation (Appendix 1) has furnished us with a correction to the profiles (Fig. 2). Comparison of the two Hall measurements before and after etching permits in fact the measurement only of the contribution of the etched layer.

The levels of doping and of real mobility thus calculated point by point are certainly superior to the averaged measured levels, since the correction allows for the abstraction of the strongly resistive and slightly doped sublayers.

For quantitative analysis of these mobility profiles it will thus be necessary to carry out this correction [11].

A correction of the doping level which is simpler but at the same time coarser has been used in certain cases. It consists in taking only the thickness of the  $n^-$  conducting layer as the sample thickness for the Hall measurements.

Since, by the Hall analysis, regions of very high resistivity of buffer layers are not measurable, we have utilized the photo-Hall effect.

### I - 3.2. Photo\_Hall

This technique is similar to the classic Hall effect but in addition carriers are generated by illumination. One can hope to deduce the mobility from it, but obviously not the number of free carriers  $n$ , which is modified by the injection light.

This type of analysis has been utilized especially by Bube /12 [12] but in a different context from ours here (essentially he studied the evolution of the mobilities with wavelength on solid GaAs).

#### - Experimental arrangement (fig. 6)

The light, here supplied by a 45W tungsten filament lamp, passes through a convergent optical system (with the interposition of the filter according to need), is reflected from a plane mirror fixed to one of the pole pieces of the electromagnet and strikes the sample.

For measurements at 77°K, the sample is placed in a windowed Dewar and immersed in liquid nitrogen. A monochromator can be added to the installation.

The same technique of successive etchings as above gives the mobility profiles in the  $n^-$  and dead layers at 300 K and 77 K (figs. 7 and 8) since for these latter the measurements had become impossible in the dark.

- Validity of the method

At first we controlled the validity of the mobilities obtained by this method by comparing them with a partially conducting layer (fig. 2).

We observe then that the light slightly increases the mobility.

Over the totality of measured samples, an increase of 5 to 20% was found in the measurements at 77 K and less than 10% for the measurements at ambient temperature

Similar effects have been demonstrated by Paesler et al. [13] for temperatures from 15°K to 80°K.

This effect, still visible at 77°K, can be interpreted as a /13 diminution of the diffusion of electrons over the ionized impurities as the illumination modifies the charge states of the traps.



At 300°K the effect of illumination is weaker because:

- first,  $\mu$  is less sensitive to  $N_D + N_A$
- second, at ambient temperature, the probabilities of thermal emission become such that the light only slightly modifies the population of the traps.

We have also determined that the variation of illumination  $\mu$  intensity does not have a noticeable effect on the mobility. remains nearly constant over a large range of illumination (approx-

imately from  $\phi$  to  $\phi/100$ ), then causes a fall to the value measured in the dark (in those cases where the latter measurement is possible) (fig. 9).

Having by these analyses gained knowledge of the principal electrical parameters of these buffer layers, it proves useful to study the nature and the behavior of the impurities present. To do this we have developed a technique for the characterization of traps in strongly resistive materials [14] (also useable for solid semi-insulators) for which capacitive methods are not applicable.

### I - 3.3. Trap spectroscopy by current transients with optical excitation

#### - Experimental method

This consists of injecting electrons and holes into the traps /14 by means of a pulsed light source and to analyze their untrapping by measuring the transient current between two contacts, ohmic if possible.

By analyzing the time constant  $\tau$  as a function of temperature, it is possible to deduce the characteristics of the traps. To facilitate the analysis we have adopted a method of signal treatment identical to that used in classical D.L.T.S. [15]. After each light pulse, the current is sampled at the instants  $t_1$  and  $t_2$ , averaged over several periods, and the difference  $\langle I(t_1) - I(t_2) \rangle$  restored in the form of spectra as a function of temperature.

Practically, this was accomplished by using the D.L.T.S. optical apparatus already existing in the laboratory [16] with the necessary modifications for current measurement (fig. 18).

The signal is treated by a HP 9821A computer. The sample is located in a variable-temperature cryostat (-200°C to +200°C) and regulation of the temperature variations is assured by the computer. The electric field created in the sample was chosen on the order of 1 V/cm.

Optical excitation can be carried out either by an electro-luminescent diode, by a He-Ne laser ( $\lambda = 0.6238 \mu\text{m}$ ) or for solid materials by a YAG laser (1.06 $\mu\text{m}$ ).

Figure 19a shows a typical spectrum obtained by this method. Parallel to the recording of the difference  $\Delta I(T)$  during the trapping, the curves of dark current and of photocurrent in the steady state are also recorded as a function of temperature for each sample (fig. 19b).

The calculations permitting the analysis of the experimental/15 results are given in Appendix 2.

This technique is, as we have said, quite close to optical D.L.T.S., but it differs from it fundamentally in that it does not require the construction of a diode on the sample surface (this diode is, on the contrary, indispensable for capacitive measurements [17]).

From the point of view of the sample, this technique is identical to TSC, but TSC is not a modulation analysis, and uses a single irreversible temperature cycle, which diminishes its electrical performance. On the other hand, the analysis for TSC is very different and more complex, and the deepest traps furthermore cannot be detected.

- Measurements

Several "high resistivity" epitaxied layers on different semi-insulating substrates have been analyzed in this manner, by using a He-Ne laser for optical excitation.

Due to the feeble penetration of the light, the measurements each time only involve a small portion of the layer, and the evolution of the spectra have been able to be followed by successive etchings down to the interface with the substrate as well as in the substrate itself.

To control the thickness of the etched material (still using the same solution 5/1/1) steps are made in the layer, then measured on the Taly Surf. Two Au-Ge contacts, separated by 500  $\mu\text{m}$ , are then evaporated onto the surface (figure 18).

Since these analyses detect deep and semi-deep levels, but /16 not levels close to bands, cathodoluminescence measurements have been carried out in certain layers with the aim, among others, to identify the shallow acceptors present.

#### I - 3.4. Cathodoluminescence

The apparatus used for this method of analysis has been described earlier [18], [19].

The luminescence of epitaxial layers of GaAs was obtained by cathodic excitation. The samples to be studied were brought to low temperature in a helium cryostat and irradiated by pulsed electron bombardment. The electron gun used for this delivered a maximum current of 100  $\mu\text{A}$  at an accelerating voltage continuously variable from 2 to 25 KV.

- During excitation, the light emitted by the sample is analyzed by a grating monochromator of 0.3 meV resolution and de-

tected by a cooled photomultiplier (56CVP) permitting operation in the infrared.

- After detection, the signal modulated at the excitation frequency is amplified by a lock-in amplifier (synchronous detector) and the spectra are recorded automatically.

- In this study, the excitation parameters (energy and throughput) were fixed at 10 KV and 20  $\mu$ A: to avoid heating the samples the width of the pulses was chosen at 1/10th of the excitation period; for example, 10 KHz and 10  $\mu$ sec, for an average power of 20 mW.

Figure 10 a gives an example of the cathodoluminescence spectrum of a lightly doped epitaxial GaAs layer.

## II - ANALYSIS AND INTERPRETATION

/17

### II - 1. Characterization of the $n^-$ layers

#### II - 1.1. Measurement of $\mu$ and $n^-$

By the classic Hall effect, we measured the residual doping, the conductivity, and the mobility of carriers in these layers and determined for each sample the respective thicknesses of the  $n^-$  and dead zones.

Over a large part of these layers the residual doping remains constant at a level between a few times  $10^{13}$  and  $10^{15}$  atoms/cm<sup>3</sup>, depending upon the sample (Table 1), then decreases at the boundary of the dead layer or substrate and becomes difficult to measure.

It should be recalled that this doping level can be controlled by the mole fraction of AsCl<sub>3</sub>.

We verified that for the corrected values of  $n$  (see I-3.1.) for the dead layer one always finds the law of dependence  $n = f(MF \text{ of } AsCl_3)$  observed in the earlier studies [4]. In fact, if we put the corrected points on the published curve (figure 3), we observe that the curve should be modified for low doping levels.

In addition to the value of  $n$ , the classic Hall effect has enabled us to obtain profiles of the mobility at 300 K and 77 K of various forms (figure 1), (the mobilities given here are electron mobilities taken to be equal to the Hall mobilities).

- at 300 K

The mobility remains nearly constant as one goes deeper into the layer, then begins to drop and the measurements rapidly become impossible.

- at 77 K

/18

At low temperature the carrier mobility is larger (multiplied by a factor of 10 or more), so one can push the measurements farther. However, in many cases they cannot be made out to the interface because of a lack of free carriers (it is not excluded that the problems encountered in these electrical measurements arise from a depletion of the rest of the layer starting from the surface).

These profiles demonstrate the presence of a more resistive region beyond the conducting zone. The relative thickness of these two layers is determined more precisely by following the evolution of the conductivity after each etch. The slope of the curve  $1/R = f(x)$  (see fig. 4), which indicates the doping at each point, remains nearly constant over most of the layer ( $n$  only varies slightly in the  $n^-$  region), then this conductivity undergoes a steep decline (about two orders of magnitude decrease). The Hall

measurement becomes impossible, and the remaining thickness is measured after the sample has been cleaved and chemically contrasted. With a correlation for the last etch carried out by extrapolation of the conductivity curve, we estimate an error of the order of 10% of the total width to be introduced in this way.

The presentation of these various characteristics: residual impurity level  $n$ , mobility  $\mu$ , mobility profiles when they exist (which are then represented by their extreme values), and thickness of the "dead" zone is made in Table I as a function of the various growth parameters.

Most of these samples have been produced by the method of classic epitaxy described in I-1.1.

Typically, for  $n$  varying between  $10^{15}$  and several times  $10^{13}/19$  atom  $\text{cm}^{-3}$ , the observed mobilities lie between 70,000 and 150,000  $\text{cm}^2 \text{V}^{-1} \text{s}^{-1}$ .

For one sample (reference 23 in Table I) of mobility 150,000  $\text{cm}^2 \text{V}^{-1} \text{s}^{-1}$  and of doping level  $n = 9 \times 10^3$  atom  $\text{cm}^{-3}$ , the total quantity of impurities  $N_D + N_A$  evaluated in this material is about  $7 \times 10^{14}$  atoms  $\text{cm}^{-3}$  (according to fig. 15), which is small and indicates a high purity material.

The correlation between the mobilities  $\mu_{77\text{K}}$  and concentrations of free carriers  $n_{77\text{K}}$  is illustrated in figure 5. One can thus see that all the epitaxial layers have high mobility at low temperatures and are therefore of good quality since they are intrinsically pure.

However, variations in compensation from one sample to another can explain the observed spread.

Notice that good results were obtained by conducting the epitaxies in argon (no's. 2, 3, 8, 11, 20 in Table I).

It is also interesting to note how one sample (No. 7), of structure ( $n^-$ /substrate  $n^+$ ), behaved. To perform the Hall measurement, the substrate had been etched away as well as a part of the epitaxial layer on the side of the  $n^-$ /substrate interface. Of the 56  $\mu m$  of the initial layer only 16  $\mu m$  remained, in which all effects of diffusion from the substrate had disappeared. A mobility of 110,000 was thus measured for a residual level of  $n$  of  $4.5 \times 10^{14}$ , giving relatively weak compensation with respect to that observed in most of the samples studied; this tends to confirm that strong compensation obtained for layers epitaxied on semi-insulators really arises from diffusion from the substrate or interface.

This is quite compatible with the cathodoluminescence results which show the presence of compensating impurities in these layers. /20

## II - 1.2. Luminescence of acceptor centers

We originally tried to identify the acceptor levels by working at 15°K. In fact, at lower temperatures, most of the conduction-band (CB) electrons are captured by donors located 5.8 meV from the CB [20], and it is difficult to distinguish transitions between neutral donors and acceptors ( $D^\circ A^\circ$ ) from transitions between the conduction band and the neutral acceptors ( $e^- A^\circ$ ) which are close in energy.

In lightly doped GaAs, ASHEN et al [21] showed that the relative intensities of ( $e^- A^\circ$ ) and ( $D^\circ A^\circ$ ) increase very rapidly between 2 and 20°K, and we have used this variation to separate these two types of transitions.

Figure 10 shows a typical example of the cathodoluminescence spectrum at 15°K obtained in a weakly doped epitaxial layer.

At high energy the spectrum is dominated by the recombination of the exciton tied to a neutral donor ( $D^0X$ ) or an ionized donor ( $D^+X$ ) at 1.512 eV, and by the annihilation of the free exciton ( $X$ ) at 1.515 eV [22].

At lower energy the spectrum consists of several emission bands which are attributed to transitions between neutral acceptors and the conduction band ( $e^-A^0$ ).

According to the recent studies of ASHEN and Bois [21], [23], the acceptor levels and their ionization energies are: carbon ( $E_A = 26.0$  meV), silicon ( $E_A = 34.5$  meV), zinc ( $E_A = 30.7$  meV), and germanium ( $E_Z = 40.4$  meV). In certain epitaxial layers we have been able to demonstrate traces of copper ( $E_A = 0.15$  eV) responsible for the ( $e^-A$ ) emission at 1.357 eV and its phonon replica [24].

#### - Study of compensation by shallow acceptors

When the epitaxial layer does not show a donor concentration profile, and certain precautions are taken, it is possible to study compensation by shallow acceptors.

Comparative measurements can be obtained by carrying out a series of successive chemical etches (with recordings of the spectra), from the surface down to the epitaxial  $n^-$ /substrate interface.

Figure 11 shows, for example, several cathodoluminescence spectra obtained in an epitaxial layer in which the free carrier concentration is below  $10^{13} \text{ cm}^{-3}$ . Aside from the exciton transitions ( $D^0X$ ) (or  $D^+X$ ) (1.511 eV), the intensity of which remains practically constant throughout the layer, the comparison of spectra at the surface (A) and near the interface (B) demonstrates an increase in intensity of the transition ( $e^-A^0$ ) with a predom-

inance for carbon.

Among others, traces of copper have been obscured in the epitaxial layer and the substrate.

In figure 12 we have represented the acceptor profiles associated with carbon and copper. From these results we can see that the rate of compensation increases near the n<sup>-</sup>/substrate /22 interface, which agrees with our hypothesis of the diffusion of impurities into the epitaxial layer.

### II. 1.3. - Diffusion model

Cathodoluminescence has thus highlighted the phenomenon of diffusion

- either from the substrate/epitaxial layer interface, where defects or impurities are accumulated at the beginning of growth
- or from the substrate itself.

When it was possible, we have utilized the profiles (x) and n(x) measured in the dark and corrected point by point (cf. I-3.1.). The corrected measurements of  $\mu_{77K}$  have since been reported on the curve given by STILLMANN et al. [26] (fig. 15).

One deduces  $N_D + N_A$  from this, point by point in the layer, and since we know corrected values for  $n = N_D - N_A$ , we obtain the  $N_A$  and  $N_D$  concentration of acceptors and donors as a function of depth.

The residual level  $N_A^0$  can be taken equal to  $N_A$  near the surface, from which one can then deduce the quantity of acceptors which have diffused from the substrate or the interface (fig. 16).

Since the profile  $N_A(x)$  is in many cases representable by the classical law in  $\text{erf}(x)$ , one can thus calculate a diffusion coefficient from it which varies between 2 and  $4 \times 10^{-11} \text{ cm}^2/\text{s}$  in agreement with DiLorenzo [7]. Note that this is a global coefficient calculated for all the acceptor impurities.

It has also been demonstrated for only certain substrates/23 (RT 304...), that there is a diffusion of shallow donors but since this effect is in general not very important no calculations have been carried out.

These diffusion processes observed in  $n^-$  material will explain in part the formation of the dead layers. It is these very layers in which we will afterwards be most particularly interested, in trying to measure their mobility and to detect the shallow and deep levels which they contain.

II - 2.1. Deposits obtained by the classical method  
a) - Mobility during illumination

In the strongly resistive zones where the classical Hall effect of our laboratory no longer gives results the mobility profiles have been obtained under illumination at 300 K and 77 K (figs 7 and 8).

All these curves fall off in the several microns preceding the interface with the substrate.

When comparing these profiles with measurements made in the dark, one observes that in a large part of the zone not measurable in the dark, the photo-Hall mobility in fact remains rather high and essentially constant (fig. 2).

This region then corresponds to a material having a very

low level of free carriers ( $N_D - N_A$ ) but also a value of  $N_D + N_A$  which is not too high since  $\mu$  remains essentially equal to the mobility measured in the non-dead  $n^-$  layers ( $\mu$  between 80,000 and 150,000 with illumination). These characteristics therefore seem /24 favorable for implantation.

On the contrary, closer to the substrate the drop in mobility reflects a real increase in the compensation of the material (drawing 17). This compensation could result from the action of deep traps or of shallow levels (acceptors), so we have first tried to identify the deep centers.

b) - Identification of the deep traps

For a large number of samples, the detrapping spectra  $I(T) = I(t_1) - I(t_2)$  were recorded as a function of temperature. Their evolution was followed with the thickness of the epitaxial layer and comparisons were carried out for the different substrates utilized.

Global analysis of the observed levels

Figures 19a) and 20) show the abundance of deep or semi-deep traps in the high-resistivity epitaxial layers.

The nature of the negative peak (Cl' in figure 20) present at high temperatures must still be studied and has not yet been well defined.

For the other levels, a peeling technique like that of DLTS has been utilized. The displacement of the spectra as a function of T when one changes the gates  $t_1$  and  $t_2$  (fig. 23) allows one to obtain the variation of the emission rate with temperature, as well as to determine the activation energy (and the capture cross section) of the center considered.

To all appearances, the observed levels were for:

- C1 - related to the presence of chromium
- C2 - tied to oxygen (A or  $E_T^L$  center) [27]  $0.75 < E_T < 0.8$  eV
- C3 - perhaps associated with  $F_e - E_T \approx 0.58$  eV /25
- C4 - this would be the  $EL_3$  center, identified in DLTS [27]
- $E_T \approx 0.55$  eV
- C5 - (difficult to peel off because it is often at the foot of another center) associated with copper  $E_T \approx 0.4$  eV (this was seen in moderately high concentration in sample  $H_{342}$  (fig. 22-1); now the analyses by cathodoluminescence have also found there a significant quantity of Cu (fig. 12).
- C6 - after comparisons with the semi-insulator, and the DLTS work 27, this can be attributed to an electron trap  $EL_6$ , up to now considered rather a crystal effect and seen in solid GaAs.  
 $0.3 < E_T < 0.34$  eV\*
- c7 - in too small a concentration - could not be peeled off.

We note that the method as it is used here (with two non-transparent contacts of identical area) do not permit one to separate the electron and hole contributions. The three centers C<sub>1</sub>, C<sub>3</sub>, and C<sub>5</sub> (cr, Fe, and Cu?) would then be traps for holes, contrary to the other levels detected.

These results are collected in figure 234 and compared with the centers identified in DLTS in conducting GaAs.

#### Evolution with depth

Two examples are given in figs. 21 a) and b) of samples studied from the surface (-1-) to the interface with the substrate (-3-).

---

\* These interpretations of the physicochemical nature of the observed traps are proposed with great reserve and require confirmation.

$C_1$  (Cu ?) is present essentially near the interface and could thus arise from a diffusion phenomenon;

$C_2$  (O ?) is observed throughout the thickness of the epitaxial layer (even when this thickness is about 10 m). Near the interface it is generally less visible because it is in the foot of  $C_1$ ;

$C_3$  (Fe ?) appears equally in the several microns above the interface.  $B_?$  27 and  $C_5$  (Cu ?) are present rather far into the layer/26 (sometimes in very low concentrations) but nevertheless appears more clearly as one approaches the substrate.

$C_6$  ( $EL_6$  ?) has been seen in all the samples; it sometimes disappears near the surface.

This shows then that a certain number of deep centers diffuse from the interface with the substrate, so that the surface layers generally show a somewhat different spectroscopy.

#### Evolution with the substrate

---

The influence of the substrate remains rather difficult to pinpoint although the appearance of the spectra seems to vary with the substrate chosen (fig. 22 - 1-2-3: 3 different substrates).

• The  $C_1$  appears in variable concentration according to the substrate while  $C_2$  is visible in great quantity in all the epitaxies (although it is sometimes masked by  $C_1$  for which the detrapping temperature is close).

• The  $C_3$  center appears weakly in many samples, but becomes very well defined in the layer H277 studied after implantation. Its concentration relative to  $C_1$  for example is larger there than anywhere else (this layer is extremely resistive).

More systematic correlations with the substrate are now under way (very distinct quantities of Cr, O and Fe).

But these results suffice to see that one has an interesting characterization tool for the deep centers, particularly for highly compensated materials.

The study of the evolution of the spectra tends to confirm the existence of the diffusion process but the quantitative aspect of the method remains difficult to study.

The role of these deep traps (essentially Cr and Fe) in the /27 compensation of the layers is undoubtedly not negligible, but one must equally take account of the large quantity of shallow acceptors which this material harbors.

To demonstrate these shallow levels several samples were analyzed by cathodoluminescence, a technique already utilized for the study of  $n^-$  materials.

c. Compensation by shallow acceptors

We have shown earlier that in those epitaxial layers of high resistivity the mobility profiles show a significant decrease near the interface. Such behavior of the mobility can only be explained by a decrease of the concentration of free carriers resulting from an increase in the rate of compensation.

It therefore seemed necessary to us to study the compensation by the shallow acceptors in these epitaxial layers. This study was made by comparing the cathodoluminescence spectra at different depths.

Figure 13 shows the spectra obtained at the surface (A) and near the interface (B) of an epitaxial layer of  $32\mu m$  width with

a dead layer of 5  $\mu\text{m}$ .

On the surface, these spectra are the same type as the  $n^-$  layer, that is, in addition to exciton transitions  $D^0X$  (or  $D^+X$ ) and  $X$  at 1.5115 and 1.515 eV, one observes recombinations ( $e^-A^0$ ) linked to the impurities C, Z, Si, and Ge. On the other hand, in the dead layer these recombinations are more efficient, with the addition of the peak at 1.36 eV attributed to singly ionized copper:  $\text{Cu}_{\text{Ga}}^+$ .

In order to correlate these results with the Hall effect /28 measurements (in the dark) we have shown on figure 14 the profiles of mobility and of the acceptors (C and Cu).

Comparison of these two profiles demonstrated the existence of a diffused zone on the order of 10  $\mu\text{m}$  thick. In the first few microns of this zone the compensation due principally to carbon increases, while the mobility drops until within the dead layer. Nearer to the interface the mobility is no longer measurable and the acceptor concentration becomes much more important.

The presence of copper at the interface and in the substrate, since it is in weaker concentrations than the other acceptors, should not play an important role in the compensation.

From these results we can conclude that the dead layer certainly results from a contamination of the epitaxial layer which took place at the start of the growth and gives rise to a diffusion process starting from the interface and/or the substrate.

### III - 2.2. Deposit obtained by low temperature growing (650°C) with a source of GaAs doped with Cr.

The classical Hall effect had already shown that the mobilities at 77°K in the  $n^-$  layers of this type were rather low (see

VIII 696 on figure 1);

For all the samples measured:

$15,000 < \mu_{77K} < 30,000 \text{ cm}^2 \text{V}^{-1} \text{s}^{-1}$  for  $n \approx 10^{14}$ . This corresponds to an increased total impurity concentration  $4 \times 10^{15} < (N_D + N_A) 10^{16} \text{ atoms cm}^{-3}$  and thus to a very strong compensation taking place spontaneously by the Cr doping from the

In the dead layers obtained practically each time with these growing conditions, the photo Hall mobility did not exceed  $35,000 \text{ cm}^2 \text{V}^{-1} \text{s}^{-1}$  (see example VIII 696 in fig. 8).

This material is still extremely resistive and has a residual/29 purity much less good than that obtained by classical growth.

The method of current transients applied to these layers did not display a spectroscopy of the deep centers very different from that of the layers at high temperatures.

In figure 22-4, the centers  $C_1$  (Cr?) and  $C_3$  (Fe?) appear more strongly than in the epitaxies with liquid source, although the  $C_2$  center is less visible. (We note however that sample H277-fig. 21-b-, even though epitaxed by the classical method, displayed a spectrum similar to that of the low temperature layers.)

In conclusion, with these different methods of characterization, we have been able to make progress in our understanding of the strongly resistive epitaxial layers. Good correlation between the drop in mobility (Hall and photoHall) and the acceptor profiles has been obtained, which tends to prove that this material has been subjected to some diffusion of compensating impurities. The contribution of the shallow acceptors would appear to be predominant with respect to that of the deep centers which are also present in the layers.

### II -3. Relative thickness of the n<sup>-</sup> and dead layers

We have seen that the most probable hypothesis rests on the development of the "dead" layer by diffusion from the substrate/epitaxial interface.

Moreover, from the point of view of the intended applications one can expect different results depending on the characteristics of the epitaxial layers (high mobility n<sup>-</sup> layers or the more or less pure "dead" layers). It is thus important to study the influence of the various growth parameters on the relative thickness of these layers in order to try to control it.

If one considers a classical diffusion of compensating impurities from the interface, and if one superimposes on this diffusion a donor concentration N<sub>D</sub> which is constant throughout the thickness of the layer but variable with p<sub>o</sub> (or with the MF of AsCl<sub>3</sub>), such a model can be represented by the scheme of Figure 25.

Now if one examines on figure 26 a set of experimental results corresponding to quite different growing conditions, one notices that this simplistic model predicts rather well the most important qualitative aspects of the phenomenon.

The spread of the results can be attributed to the influence of the ensemble of growth parameters. The principal parameters (vector gas: H<sub>2</sub> or Ar, growth temperature T<sub>D</sub>) are represented by different symbols.

We will examine successively the influence of each of these.

First, one can expect a priori in a diffusion process that the growth temperature should have a dominant effect. This does not seem to be the case, particularly since we have studied the influence of this parameter over a wide range of values (T<sub>D</sub> varies from 650 to 750°C). Even though the studies of low temperatures (symbols • and \*) led to the smallest thicknesses of the dead

layers (that is, to a limited diffusion of compensating impurities), one notes that the influence of the temperature is not very pronounced. It is to be regretted, however, that the other parameters had not been held strictly constant.

A second parameter is the growing time. Our experiments, of /31 which the duration varied from 30 minutes to 2 hours, did not permit the effect to be displayed.

Another factor to be considered is the substrate, which could act as a source of impurities. The studies presented in figure 26 were carried out on 6 different substrates obtained from various sources. Even though at times we were able to see a noticeable difference in the thickness of the "dead" layer for the different substrates utilized in the course of a single growth (see Table I), we could not systematically associate a value of the thickness of this layer with the use of a given substrate.

However, if one presents the results obtained with two extreme types of substrates (figure 27), that is, the "least diffusing" (A) and the "most diffusing" (B), a marked difference is observed. Furthermore, one should notice that the dominant compensating element in the diffusion is not chromium, or at least not only chromium, since substrate A contained much more of this element than did B but gave a smaller thickness of the dead layer.

It is also possible to imagine that the source of the diffusion is not from the volume of the substrate but from impurities present on its surface. The variation in the concentration of compensating impurities could also result in part from the transient rebuilding phase of the growth period.

These latter two hypotheses seem to be contradicted by experiment when one examines the results of a series of studies carried out under the following conditions (fig. 26 - symbol +): the

the operating mode was identical to that of a normal growth process, only the conditions of establishment of the growth regime were modified. For this, the growing conditions were stabilized by superimposing on the flow of growth materials (flow of H<sub>2</sub>, As Cl<sub>3</sub>) carrier toward the source of Ga [4] a flow of etchant AsCl<sub>3</sub> which did not pass the source and which dissociated thermally to give HCl. With conditions properly adjusted, the substrate was held at zero growth for 30 minutes, to permit sufficient stabilization of the conditions of deposition. One notes in this case that the thickness of the dead layer is at a mean value and rather high. One can thus not accept the two hypotheses presented above.

In conclusion, the thickness of the dead layer depends primarily on the level of residual doping, to a lesser degree on the growth temperature and the substrate, and relatively little on the growing time. /32

Knowing the influence of these parameters, one can choose the growing time to have either only a dead layer or a dead layer on top of an n<sup>-</sup> layer.

### III - IMPLANTATION

Studies were undertaken to test the behavior of the high-resistivity layers during thermal ion-activation treatments and to determine the characteristics of the implanted layer.

The implantations were carried out by:  
Messrs. Favennec and Pelous of CNET (Lannion)  
Mr. B. Sealy of the University of Surrey (U.K.)  
whom we thank for their cooperation.

#### a) Thermal treatments of the n<sup>-</sup> layers

Two types of thermal treatment were carried out:

- non-encapsulated sample annealed in a purified hydrogen atmosphere for one hour at 750°C,
- sample encapsulated in  $\text{Si}_3\text{N}_4$  annealed under purification argon for 15 minutes at 850°C.

Table II summarizes the results schematically for the various epitaxial layers.

One sees the formation of a p-type surface layer in the two cases considered. This transformation is analogous to that already mentioned with respect to other samples of GaAs, and in particular of solid crystalline GaAs: Cr. A center situated at  $E_V + 110$  meV, of unknown origin, is responsible for this transformation [28].

b) Implantation of the active layer

/33

$\text{Se}^+$  ions were implanted under rather different conditions in the two laboratories, as illustrated in Tables III and IV, and in the electrically active or "dead" layers.

The results are presented in Table IV. In most of the studies, the very small sample sizes did not permit detailed characterization; one observes a number of common points between the samples:

- the mobility of the active layer is rather constant and essentially identical to that found for the implanted chromium-doped substrates;

- the doping levels and the thicknesses are close to those expected, while the electrical activity is very high (the fact that they appear to be higher than 100% is probably due to errors in the determination of  $n$  and  $e$ ). This result however is marked-

ly different from that found in the chromium-doped substrates, for which the electrical activity is generally weaker. The greater purity of the epitaxial material may permit this result to be explained, whether it comes from an active or a "dead" layer.

An analysis of the  $n^-$  layer under the implanted zone was carried out on a Hall sample. Figure 28 shows the general shape of the mobility profile under the active layer. Comparison with a mobility profile characteristic of an  $n^-$  layer brings out a noticeable reduction of the mobility in the case of an implanted layer.

Some samples even give values more representative of type p than type n. One can thus conclude that the thermal activation treatments have an effect on the high resistivity layer, but it is difficult to separate the phenomena related to the outward diffusion of acceptors from the substrate and those caused by surface conversion. The active layer does not seem particularly affected by the two diffusion mechanisms.

#### c) - Results of devices

One of the samples was held for a technological treatment. Unfortunately the choice was made only on the basis of maximum usable surface and not as a function of the results of the characterizations.

The performance of a low noise FET obtained is presented in Table VI, in comparison with an identical implantation in a solid substrate, and for a grid length of 0.8  $\mu\text{m}$ . One can see a noticeable improvement in all the values, which can be attributed to the use of an epitaxial layer of high resistivity and purity.

## CONCLUSIONS

/35

In employing either classical or low temperature epitaxial growth techniques, experimented with for several years in our laboratory, we have shown that it is possible to control the formation of layers of medium or high resistivity.

To characterize these layers, some new techniques had to be developed in order to study, as a function of thickness, the evolution of mobilities by photoHall and spectroscopy of shallow and deep centers by cathodoluminescence and current transients.

These techniques revealed two layers:

- one very pure of medium resistivity and high mobility ( $\mu_{77K} > 100.000 \text{ cm}^2 \text{V}^{-1} \text{s}^{-1}$ ),
- the other, farther from the surface, of elevated resistivity ( $\rho > 10^3 \Omega \cdot \text{cm}$ ), called the "dead" layer.

The strong compensation of this latter layer could be explained solely by the diffusion of shallow acceptors, and principally of carbon, from the substrate or the interface. Moreover the presence of deep traps (Cr, O<sub>2</sub>, Fe), the analysis of which is so far purely qualitative, comes again to reinforce this aspect. Other impurities were detected toward the interface with the substrate, such that copper also has a diffusion profile in the epitaxial deposit.

We have seen that the highly resistive layer can remain rather pure however ( $N_D + N_A \approx 10^{15} \text{ atom cm}^{-3}$ ) over several microns, which appears interesting for implantation.

For the layers obtained at low temperature with a source of GaAs doped with chromium (thus with a voluntary compensation which is added to the substrate effects), the purity is markedly lower.

The effects of the principal parameters of the diffusion /36 (temperature, time, nature of the substrate) having been determined, it is now possible to choose the growing time and the residual doping (a function of the mole fraction of  $\text{AsCl}_3$ ) to obtain layers of the desired resistivity and purity.

Several tests of the implantation of  $\text{Se}^+$  in the high resistivity layers were carried out in collaboration with CNET and the University of Surrey.

The performance of the first FET devices obtained from these implanted layers shows a marked improvement with respect to direct implantation in the substrate (2.6 dB of noise at 10 GHz as compared with 3.4 dB at 8 GHz).

## BIBLIOGRAPHIC REFERENCES

1. M. Berth, M. Cathelin, G. Durand, IEDM, (Washington) December 1977.
2. D. Boccon-Gibod, G. Durand, 2nd Europ. Sol. St. Circ. Conf. (Toulouse 9, 1, 88 (1976).
3. D. Boccon-Gibod - CNET Report No. 74-9-B-492 (1976).
4. L. Hollan - Proc. 5th Int. Symp. GaAs (Deauville) Inst. Phys. Conf. Ser. no. 24, 22 (1975).
5. H. M. Cose, J.V. di Lorenzo, Proc. 6th Int. Symp. GaAs (Saint Louis) Inst. Phys. Conf. Ser. no. 33b, 11 (1977).
6. J. Hallais et al. J. Electroch. Soc. 124, p. 1290 (1977).
7. J. V. Di Lorenzo, G. E. Moore, J.E.S. 118, 1824 (1971).
8. L. Hollan, A. Mircea, Proc. 4th Int. Symp. GaAs (Boulder) Inst. Phys. Conf. Ser. No. 217 (1973)
9. T. Nozaki, M. Ogawa, H. Watanabe, Proc. 5th Intst. ymp. GaAs (Deauville). Inst. Phys. Conf. Ser. no. 24, 46 (1975).
10. Van der Pauw- Philips Res. Reports 13, 1-9 (1958).
11. J. F. Proth et J. Monnier, Grenoble, Colloquium on Characterization 603 (1972).
12. R. H. Bube, H. MacDonald J.P.C.S. 22, 173-180 (1971). A. Lin, R.H. Bube J.A.P. 47, 1859, (1976).
13. M. A. Paesler - M.J. Queisser, Sol. St. Com. 21, 1143 (1977)
14. Ch. Hurtes, M. Boulou, A. Mitonneau, D. Bois, To be published in...A.P.L.
15. D.V. Lang, J.A.P. 45, 3023 (1974).
16. A. Mitonneau, G. M. Martin, A. Mircea, Elect. Let. 13, 666 (1977)
17. C. T. Shah, L. Forbes, L. Rosier, A. F. Tasch Jr., Sol. St. Elect. 13, 759 (1970).
18. M. Boulou, D. Bois - To be published in J.A.P.
19. M. Boulou, Rapport LEP ref. MB/D.L. - JC CRL 198/11-B295.

20. C. J. Summers, R. Dingle, D.E. Hill, Phys. Rev. B1, 1603 (1970).
21. D. J. Ashen, P. J. Dean, D.T.J.Hurle, J.B. Mullin, A.M. White J. Phys. Chem Solids, 36, 1041 (1975)
22. E. H. Bogardus, H.B. Bebb, Phys. Rev. 176, 993 (1968)
23. D. Bois, D. Beaudet, J.A.P. 46, 3882 (Sept. 1975).
24. H. J. Queisser, C. S. Fuller, J.A.P. 37, 4895 (1966).
25. C. Schiller, M. Boulou, Philips Technical Review 35, 329 (1975)
26. G.E. Stillman, C.M. Wolfe: "Characterization of epitaxial semicond. films" - H. Kressels ed., 70 (1976).
27. A. Mircea, A. Mitonneau, G.M. Martin, DGRST Report no. 75-7-1484.
28. J. Hallais, A. Mircea-Roussel, J.P. Farges, G. Poiblaud GaAs and related compounds (St. Louis), 220 (1976) Inst. of Physics Conf. Ser: no. 33b.

ORIGINAL PAGE IS  
OF POOR QUALITY

TABLE I

Nos	Growth Nos. H...	$\mu$		WTK profile (1)		Thickness of or dead layer ( $\mu$ )	$T_d$ (2) $^{\circ}C$	vector gas(2)	Remarks
		(as/cm <sup>2</sup> )	(as/cm <sup>3</sup> )	( $\times 10^{-3}$ )	( $\times 10^{-3}$ )				
1	344	• 10 <sup>15</sup>	72.000	75-77	68	15	3	720	H <sub>2</sub>
2	328	• 10 <sup>14</sup>	76.000			18	2	650	Ar
3	323	• 10 <sup>14</sup>	93.000			7	7	720	Ar
4	366	• 10 <sup>14</sup>	93.000			18	4		
5	372	• 10 <sup>14</sup>	86.000			12	4		
6	270	• 10 <sup>14</sup>	76.000	76-77	39	8	2		
7	360	• 10 <sup>14</sup>	110.000			16			
8	329	• 10 <sup>14</sup>	116.000			5	1	650	Ar
9	363	• 10 <sup>14</sup>	95.000	93-97	68	20	1		
10	364	• 10 <sup>14</sup>	91.000	91-92	22	2	2	650	Ar
11	293	2.5.10 <sup>14</sup>	141.000			16	2		
12	350	2.10 <sup>14</sup>	115.000	115-97	8	6	3	710	H <sub>2</sub>
13	371(a)	1.1.10 <sup>14</sup>	110.000	110-97	27	2.5	2.5		
14	271(a)	1.2.10 <sup>14</sup>	110.000	110-97	3	10	10		
15	340	1.1.10 <sup>14</sup>	119.000	119-91	13	1			
16	371(b)	10 <sup>14</sup>	118.000	118-91	5	8	8		
17	371(c)	7.6.10 <sup>13</sup>	120.000	120-91	9	5	5		
18	272	7.10 <sup>13</sup>	110.000	110-97	5	6	6		
19	363	7.10 <sup>13</sup>	120.000	120-91	5	7	7		
20	214	6.10 <sup>13</sup>	120.000					720	Ar
21	376	5.10 <sup>13</sup>	115.000	125-97	3	6.5			
22	314(a)	2.10 <sup>13</sup>	126.000	128-97	5	7	7		
23	332(b)	• 2.10 <sup>13</sup>	120.000	150-91	4	6	6		

15.. (1) The profile is given in terms of the extreme values:  $\mu$  initial (sample not etched) —  $\mu$  final (last etch at which measurement was still possible).  
 16.. (2) Wherever nothing is listed, the conditions are  $T_D = 750^{\circ}C$  under H<sub>2</sub>, with growth on a semi-insulating substrate.

ORIGINAL PAGE IS  
OF POOR QUALITY

TABLE II

Sample	Growth	Annealed in H <sub>2</sub>	Annealed encapsulated
H 268	'High temperature'	$\rho \sim 10^{16}$	-
H 289	High temperature	-	$\rho \sim 10^{15}$
S 695	'Low temperature'	$\rho \sim 10^{16}$	-

Table III

Initial samples				
N°	Growing conditions	n 77 °K (nt/cm <sup>3</sup> )	$\mu$ 77 °K (cm <sup>2</sup> V <sup>-1</sup> s <sup>-1</sup> )	Thickness (μm.)
H 271	High temperature	$3,3 \cdot 10^{14}$	70.000	10
H 277	High temperature	not measured	-	8
H 289	High temperature	$1,5 \cdot 10^{14}$	93.000	3,5
S 694	Low Temperature	not measured	-	4,2
S 696	Low temperature	not measured	18.000	4,5

ORIGINAL PAGE IS  
OF POOR QUALITY

Table IV  
Implantation

Sample	Ions	Implantation	Ion	Dose <sup>a</sup> (cm <sup>-2</sup> )	Temperature (°C)	Encapsulant	Energy <sup>a</sup> (keV)	Thermal activation, treatment
H 271		CNET	Se <sup>+</sup>	2,5 10 <sup>13</sup>	400	Si <sub>3</sub> N <sub>4</sub> 1000 Å	400	900° /Argon/ 20 min.
H 277		Univ. Surrey	"	1,5 10 <sup>12</sup>	200	"	250	850° /Argon/ 15 min.
H 289		Univ. Surrey	"	"	200	"	250	850° /Argon/ 15 min.
8.694		CNET	"	2,5 10 <sup>12</sup>	400	Si <sub>3</sub> N <sub>4</sub> 1000 Å	400	900° /Argon/ 20 min.
8.696		CNET	"	"	400	"	400	900° /Argon/ 20 min.

sample.	(Hall measurement.)			(E(V) measurement)			(Electrical activity %)		
	n(cm <sup>-3</sup> )	A 300°K (cm <sup>2</sup> V <sup>-1</sup> S <sup>-1</sup> )	NS	n(cm <sup>-3</sup> )	e(Å)	V <sub>B</sub> (Volts)	NS	Hall	C (V)
H 271	-	-	-	1 10 <sup>17</sup>	2100	2.3	2,1 10 <sup>12</sup>	-	110
H 277	1 10 <sup>17</sup>	3060	1,5 10 <sup>12</sup>	1 10 <sup>17</sup>	2200	4	2,2 10 <sup>12</sup>	100	140
H 289	1,2 10 <sup>17</sup>	3340	2 10 <sup>12</sup>	1,5 10 <sup>17</sup>	2000	3,5	3 10 <sup>12</sup>	130	200
8.696	-	-	-	8 10 <sup>16</sup>	2000	1,8 2,5	1,6 10 <sup>12</sup>	-	90

ORIGINAL PAGE IS  
OF POOR QUALITY

TABLE VI

Ion implanted	Implantation substrate	FET Result			
		f MHz	NF dB	G mV/m	NF dB
Se <sup>+</sup>	GeAs: Cr	8	3,4	7,2	
Se <sup>+</sup>	n <sup>-</sup> layer	10	2,5	6,6	

FIGURE CAPTIONS

/43

Fig. 1. Mobility profiles in the  $n^-$  layer measured at 300K and 77 K (samples not illuminated)

Fig. 2. Mobility profiles relative to the same epitaxial layer -measured; - in the dark  
- corrected for the contribution from the "dead layer"  
- under illumination

Fig. 3. Residual doping levels obtained as a function of the mole fraction of  $AsCl_3$  utilized (compared with curve published at Deauville) [4]

Fig. 4. Evolution of surface conductivity across the layer (measured after each etch):  $1/R_D = f(x)$ .

Fig. 5. Correlation between the measured mobilities at 77K and the residual doping levels.

Fig. 6. Experimental arrangement for PhotoHall measurements.

Fig. 7. Mobility profiles under illumination obtained at 300K (low - temperature growth - source solid GaAs.)

Fig. 8. 77K mobility profiles with illumination (most samples epitaxed at high temperature ( $750^\circ C$ ) with a liquid Ga source).

Fig. 9. Effect of illumination intensity on PhotoHall mobilities.

Fig. 10 a) Cathodoluminescence spectrum at  $15^\circ K$  for an  $n^-$  layer epitaxed on semi-insulator substrate. (The shoulder at 1.493 eV marked X represents an acceptor ( $E_A = 22$  meV) not yet identified in GaAs [23]).  
b) Spectrum of the same sample at lower energy, showing the conditions electron-acceptor recombination band ( $e^-A^0$ ) at 1.36 eV, attributed to singly- ionized copper:  $Cu_{GA}^{+}$ , and its phonon replica ( $\hbar_{WL_O} = 36$  meV) at 1.324 eV.

Fig. 11 Evolution of cathodoluminescence spectrum with depth in a  $12 \mu m$  thick.  
A - at the surface; G - close to  $n^-$ /substrate interface

Fig. 12 Profile of shallow acceptors in an epitaxial  $n^-$  layer obtained by tracing the maximum intensity of the carbon and copper luminescence as a function of depth.

Fig. 13 Evolution of the cathodoluminescence spectra at the surface (A) and near the interface (B) in an epitaxial layer  $32 \mu m$  thick, 5  $\mu m$  of which is dead layer. /44

Fig. 14 Profiles of mobility (dark) and of shallow acceptors (carbon and copper) in the same sample (fig. 13)

- full dashes: mobility
- dash-point: maximum intensity of electron-acceptor recombination ( $e^-A^\circ$ ) with carbon
- light dashes: maximum intensity of electron-acceptor recombination ( $e^-A^\circ$ ) with copper.

This figure demonstrates the rise in compensation corresponding to the drop in mobility in the diffused zone.

Fig. 15 Curve of Stillman 26 giving the total quantity of impurities in a homogeneous epitaxial layer as a function of mobility measured at 77K with a 5 KG magnetic field.

Fig. 16 Profile of diffusion of acceptors from the substrate (or the interface):  $N_A(x)$   
- evolution across the buffer layer of the total quantity of donors and acceptors  $N_D(x)$  and  $N_A(x)$ .

Fig. 17 Schematic representation of the most frequently obtained structure for a "buffer" layer epitaxed on a semi-insulator.

Fig. 18 Arrangement for trap spectroscopy by current transients with optical excitation.

Fig. 19 Typical spectra obtained (sample VIII 726/RT 281)  
(a)  $I(T)$  - transient current as a function of temperature  
-(centers  $C_1$ (Cr?),  $C_3$ (Fe?),  $C_6$ (EL6))  
(b)  $I(T)$ : dark current and photocurrent in steady state vs. temperature

Fig. 20 Sample containing a large number of differentiable centers (H 274/RT 326)  $C_2(O_2)$ ,  $C_4(B?)$ ,  $C_5(Cu?)$ ,  $C_6(EL6)$ .

Fig. 21 Evolution of deep centers with depth (from the interface with the substrate -1- to the surface -3-) for two samples epitaxed at high temperatures:  
a) H 282/RT 304 (12 $\mu m$  thick)  
b) H 277/RT 326 (7 $\mu m$  thick)

Fig. 22 Spectroscopy of deep centers for the following samples:  
1 - H342/Laser diode (layer not "dead")  
2 - H 283/SUMITOMO 20336 }  
3 - H 237/RT 281 } "dead" layers  
4 - VIII 726/RT 281 }  
(Note that samples 3 and 4 are epitaxed on the same substrate by two different growing methods)

Fig. 23. Evolution of peaks as a function of the time of the gates/45  
 $t_1, t_2$  ( $\frac{t}{T}$ ,  $\frac{V}{V_s}$ )

Fig. 24. Variation of the rate of emission from the traps (in fact here  $T^2/e$ ) with temperature  
- comparison of the results of this study (dotted) and those obtained in DLTS for conducting material (solid curve).

Fig. 25 Model justifying the existence of a dead layer by the evolution of the acceptor and donor levels with thickness.

Fig. 26 Evolution of the thickness of the dead layer with residual doping n (points from experiment).

Fig. 27 Same evolution as in fig. 26, but for samples epitaxied on two very different types of substrates.

Fig. 28. Mobilities compared for a buffer layer which is  
- under an  $n^+$  epitaxied layer  
- under an  $n^+$  implanted layer

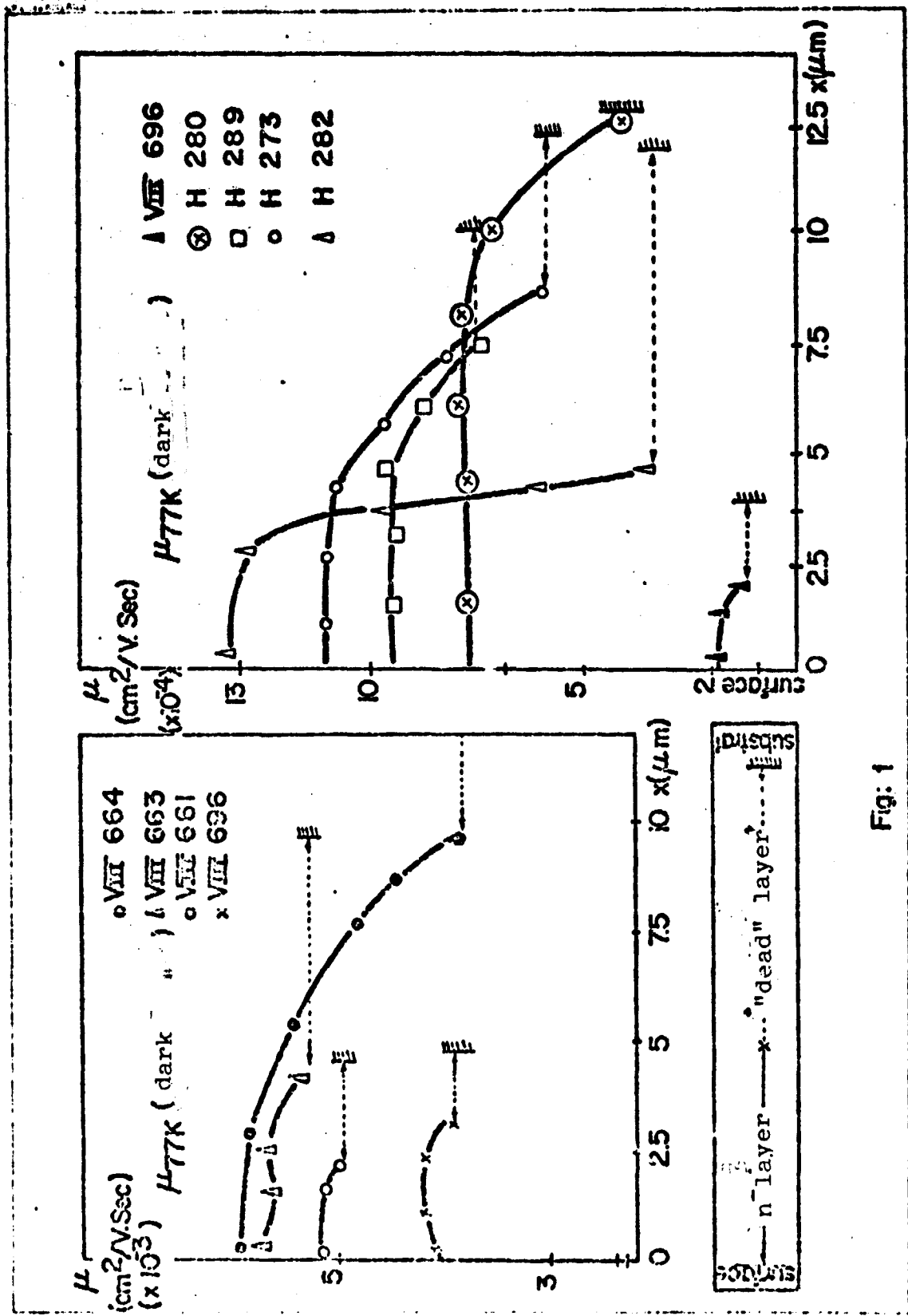


Fig. 1

ORIGINAL PAGE IS  
OF POOR QUALITY

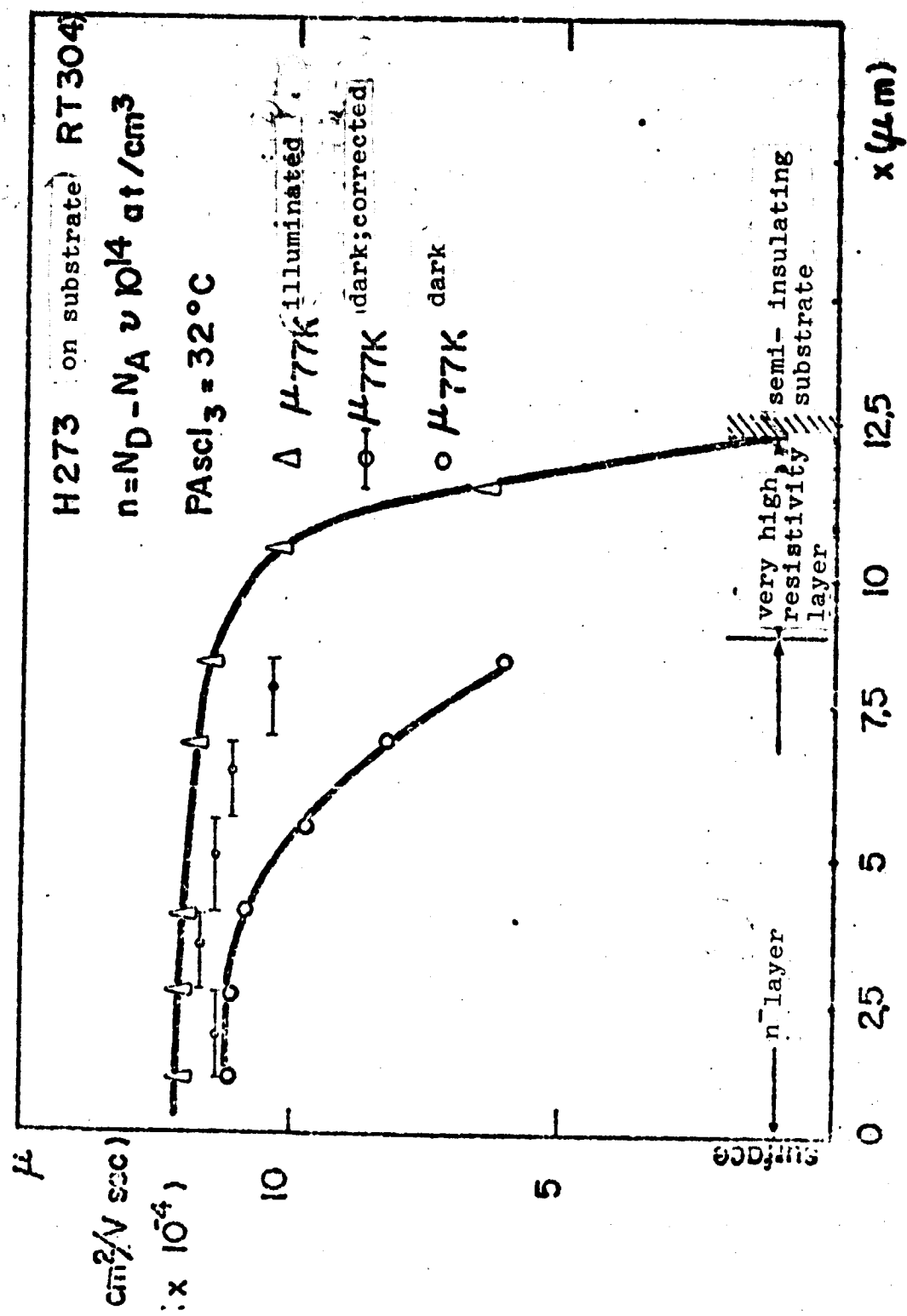


Fig. 2

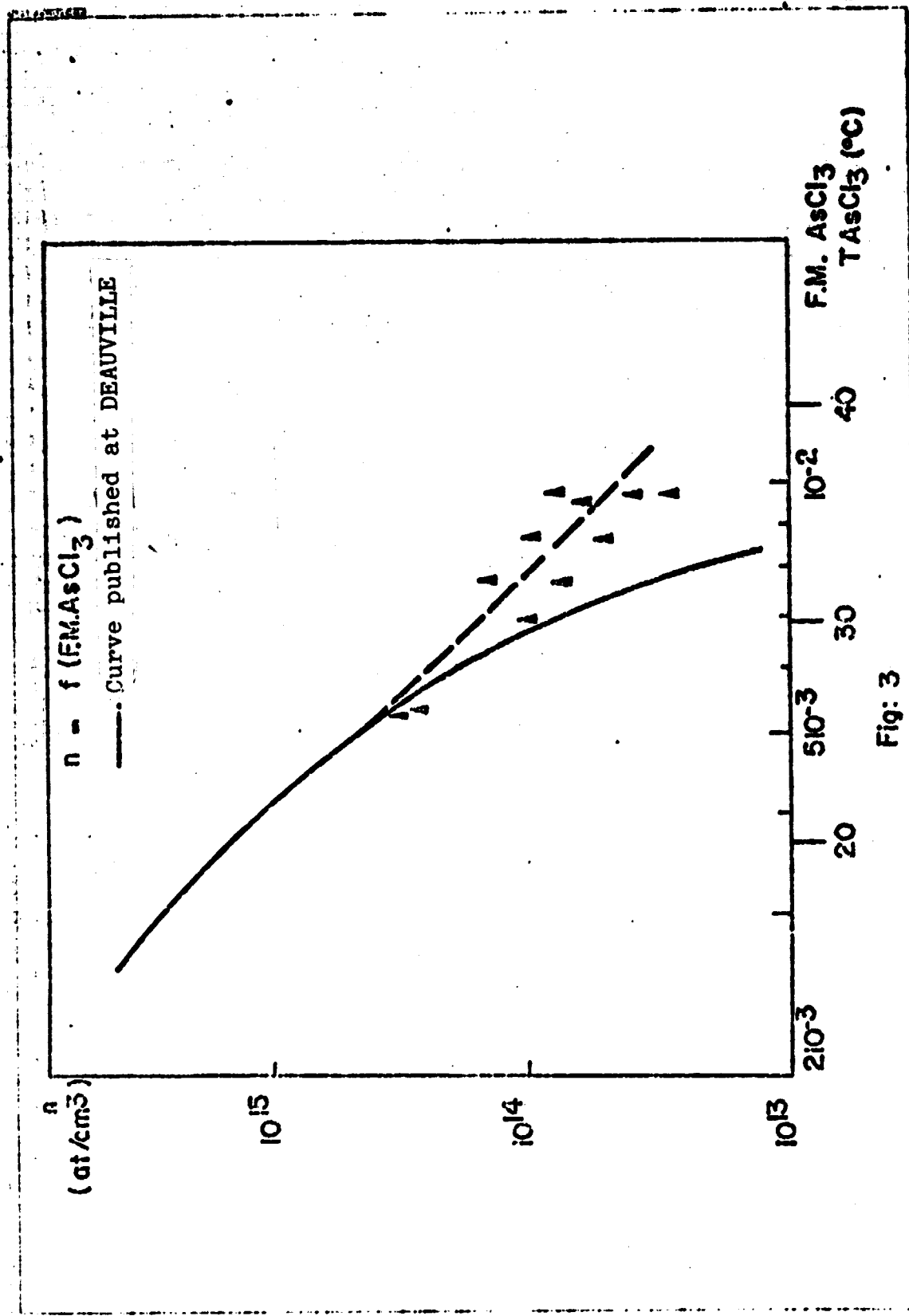
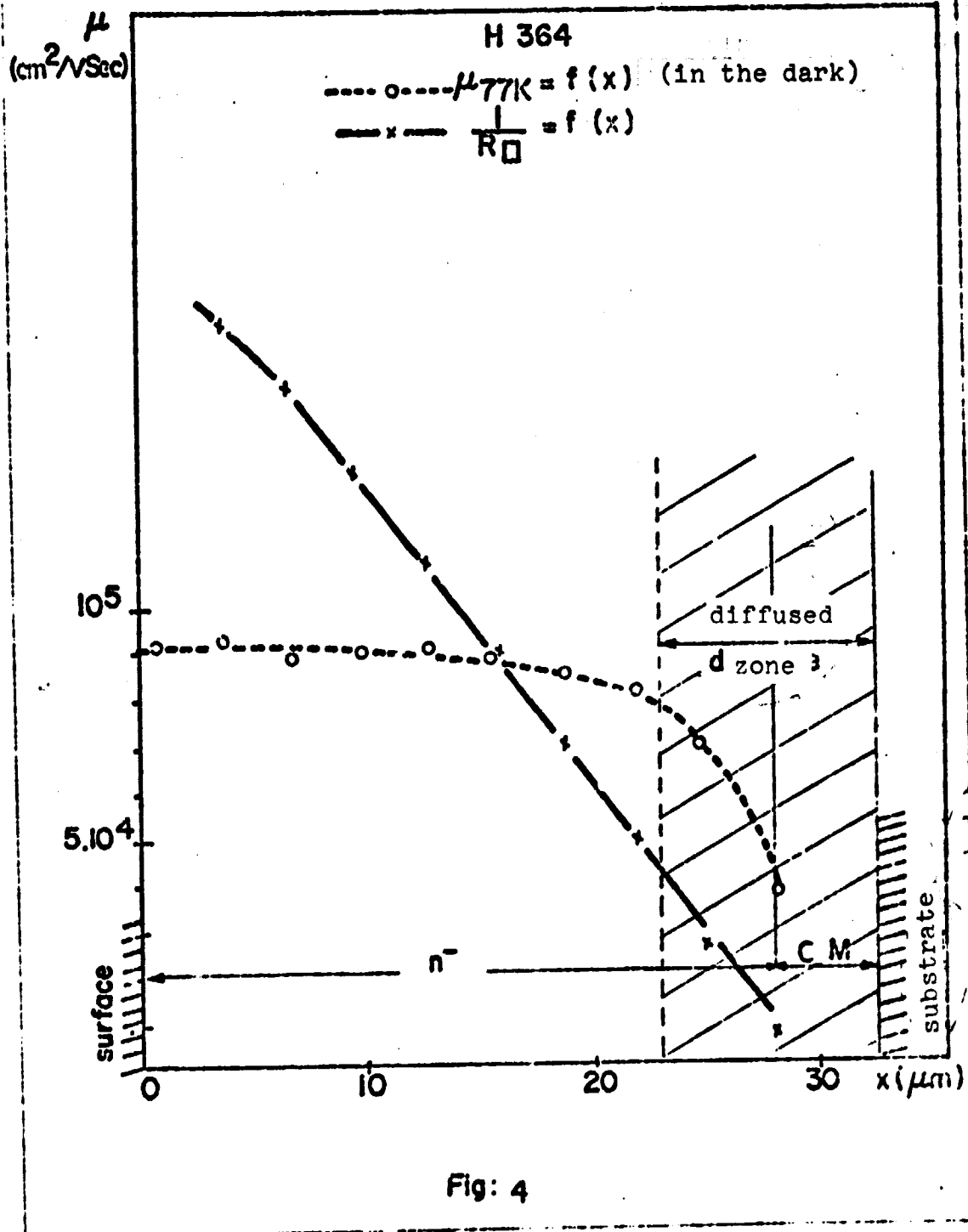


Fig: 3



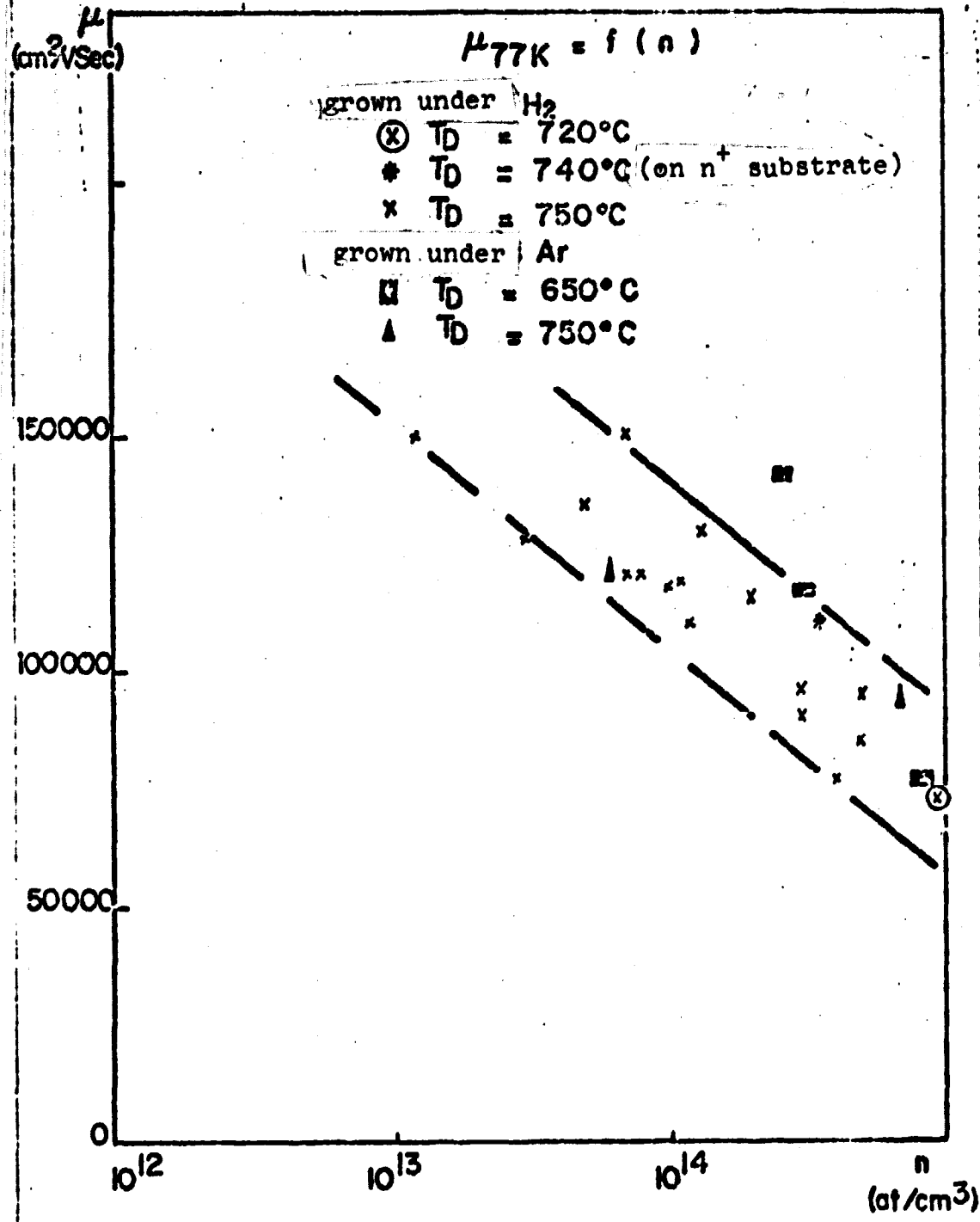
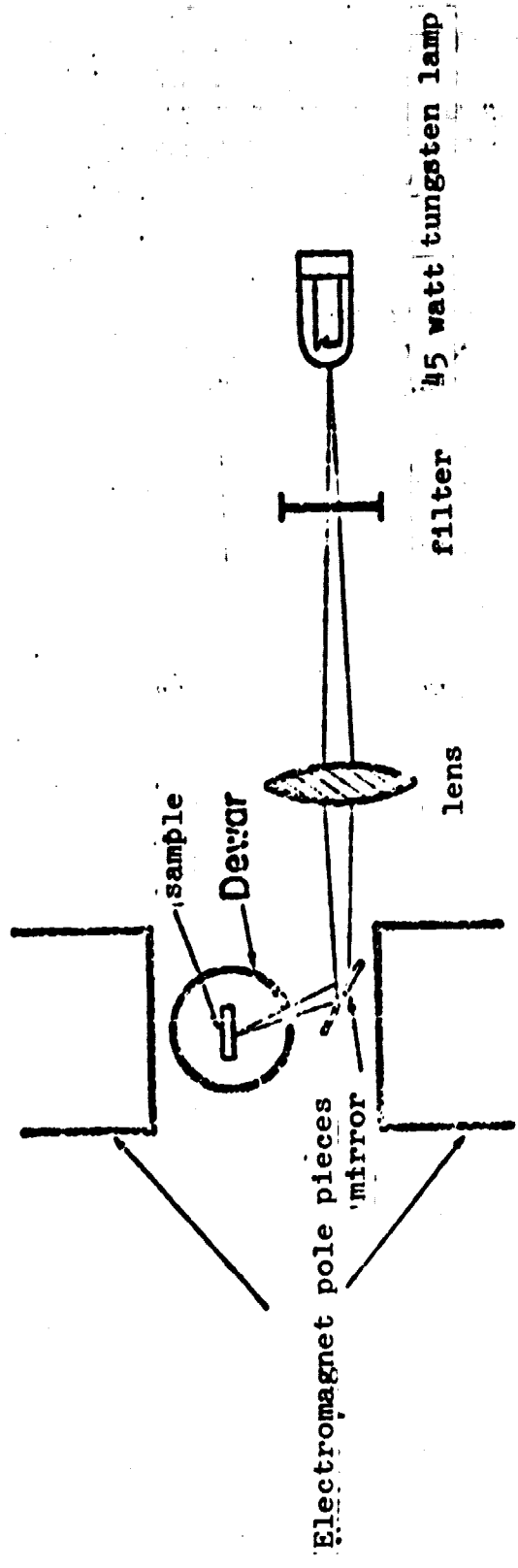


Fig: 5



ARRANGEMENT FOR PHOTOHALL MEASUREMENTS

Fig: 6

Fig: 7

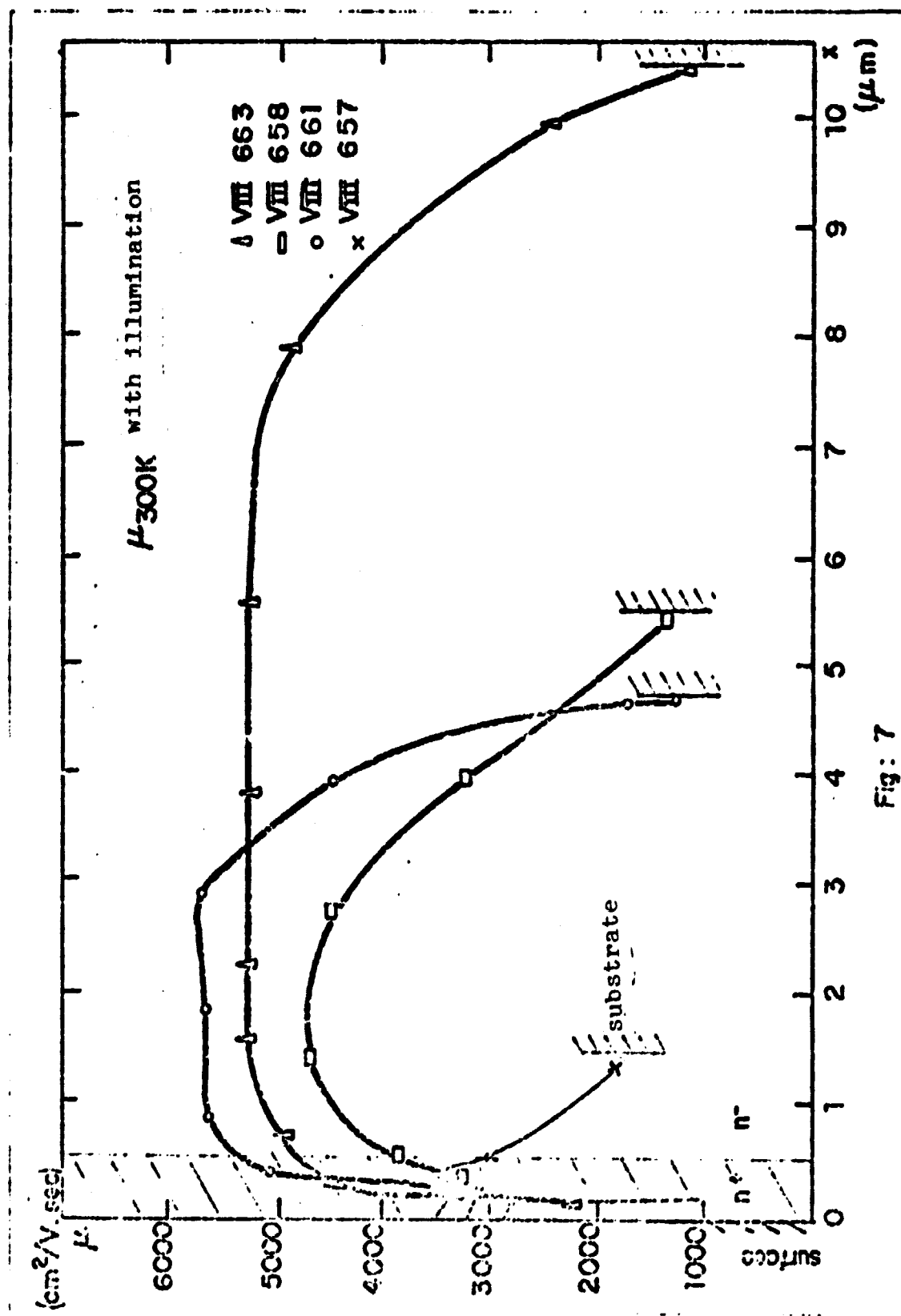
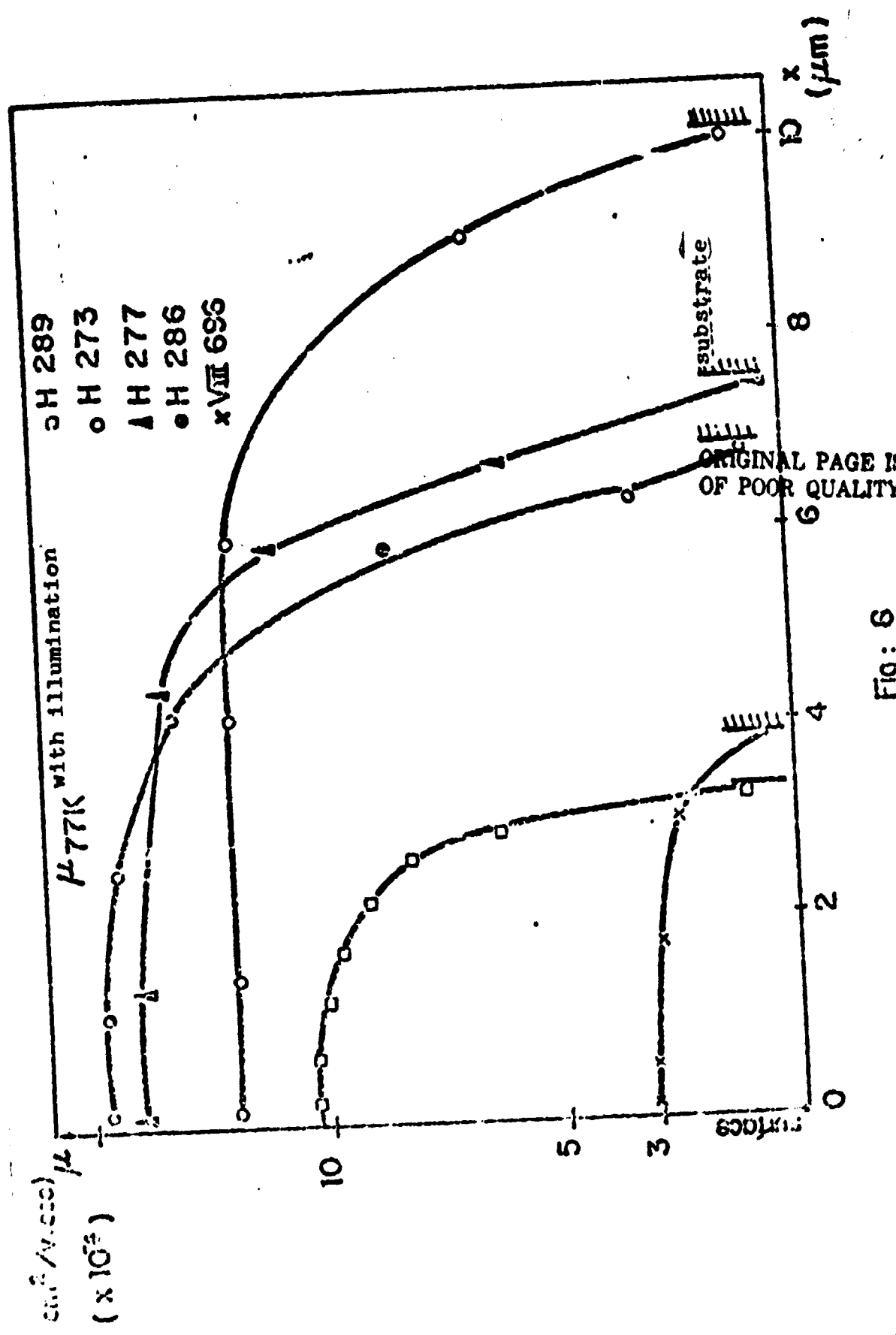


Fig: 6



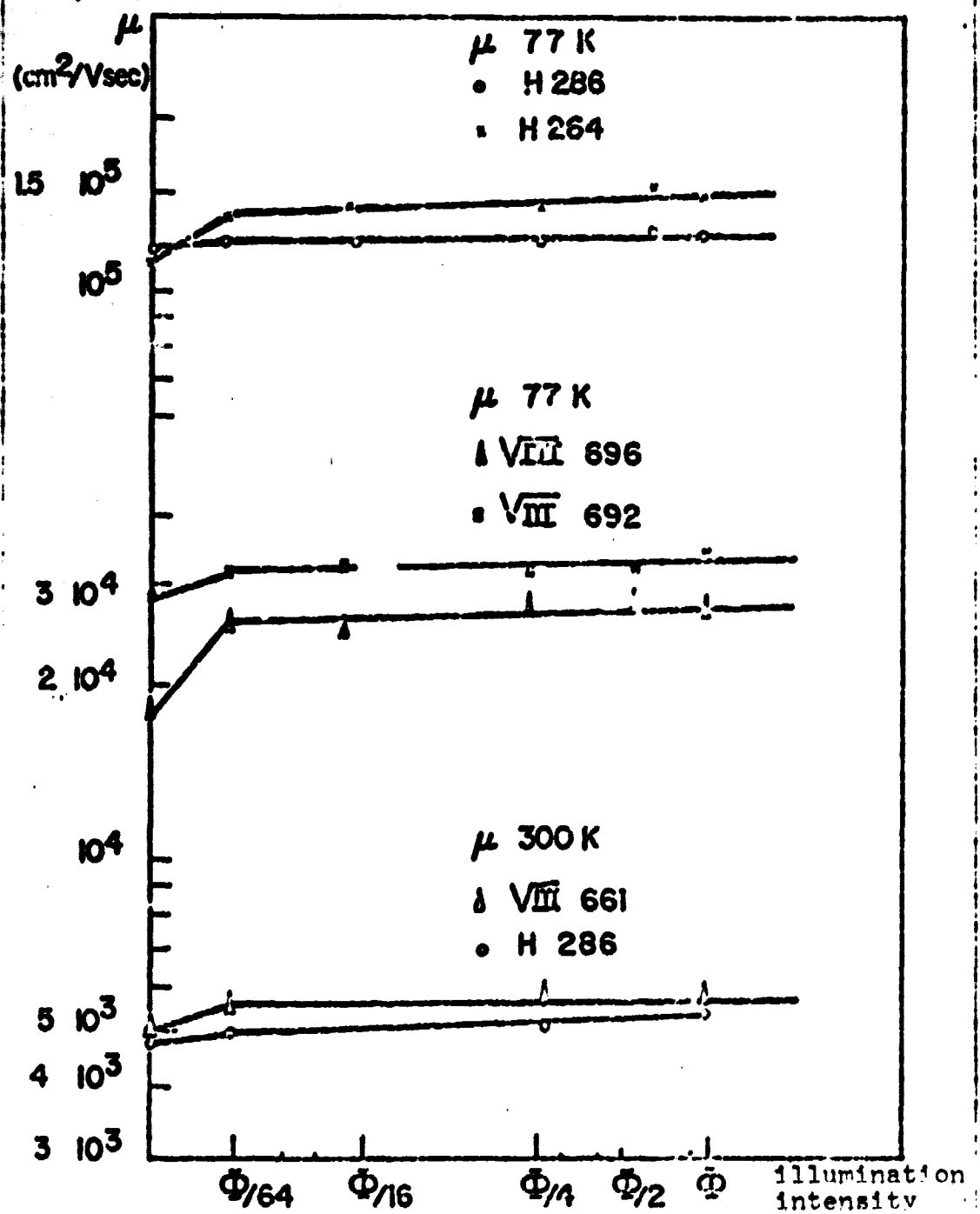
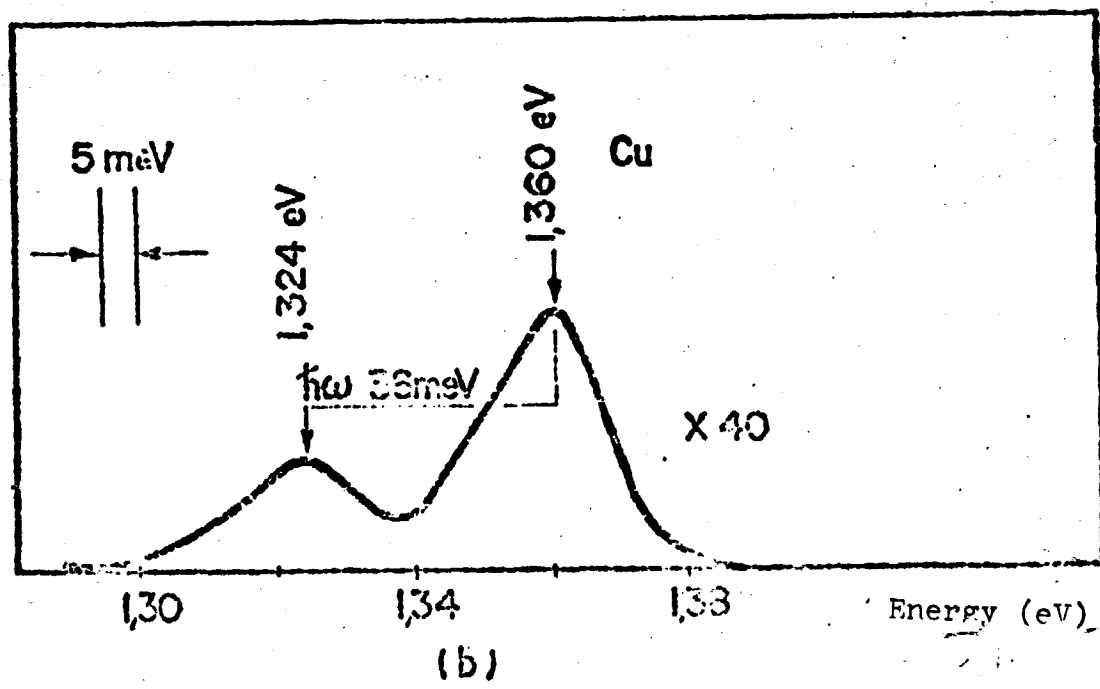
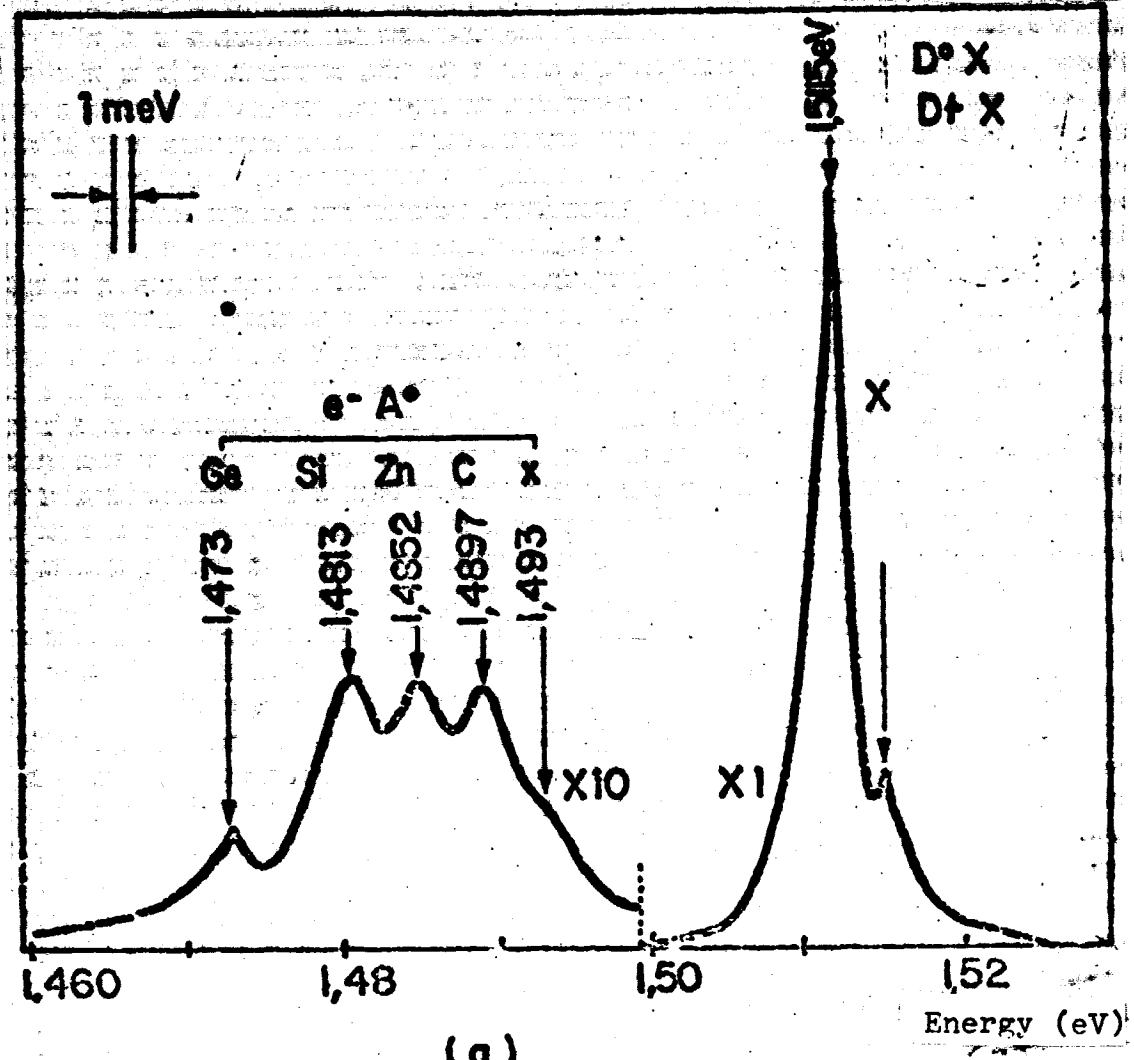


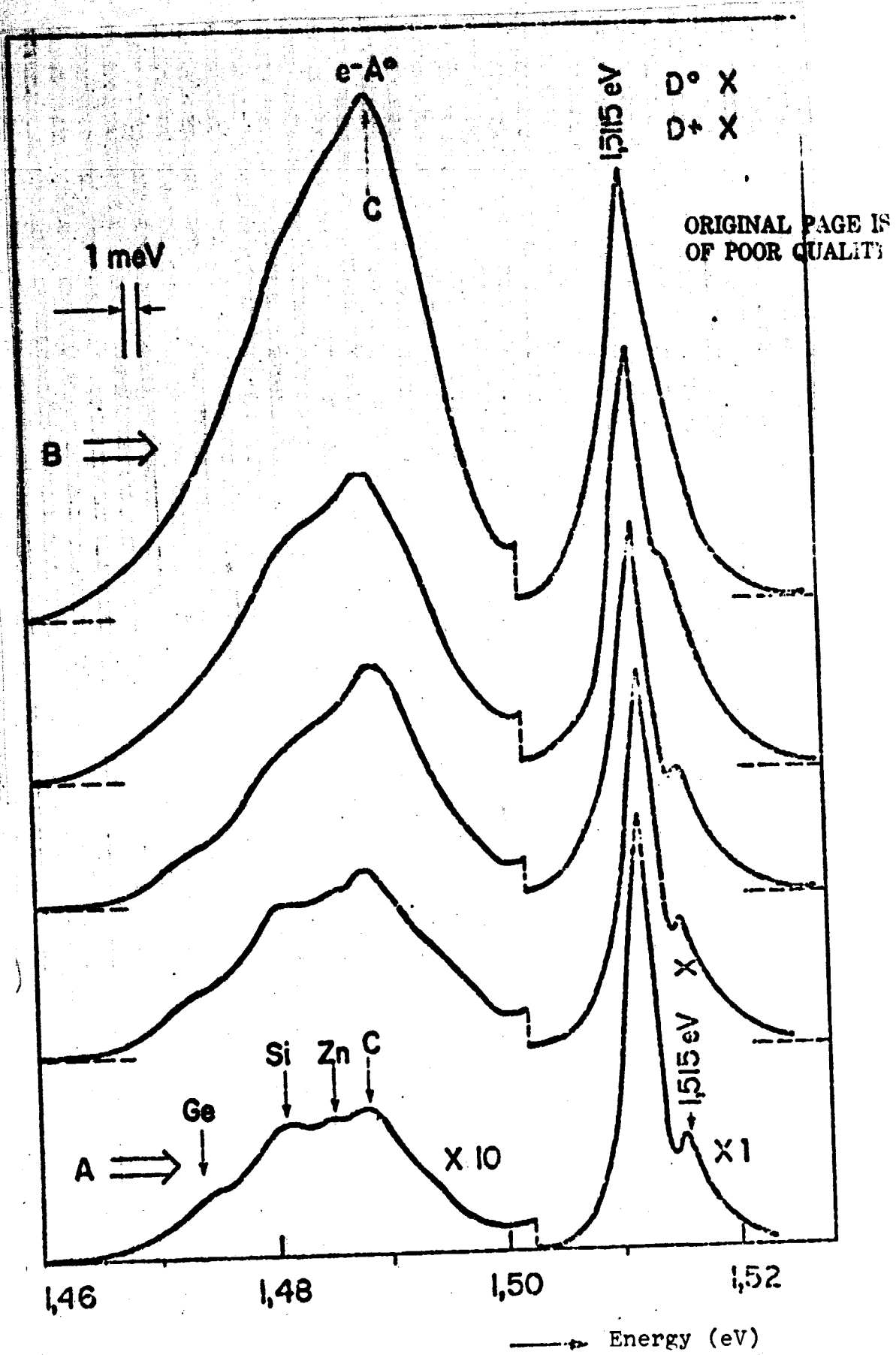
Fig: 9

(arbitrary units)

Luminescence Intensity (arbitrary units)



Luminescence Intensity



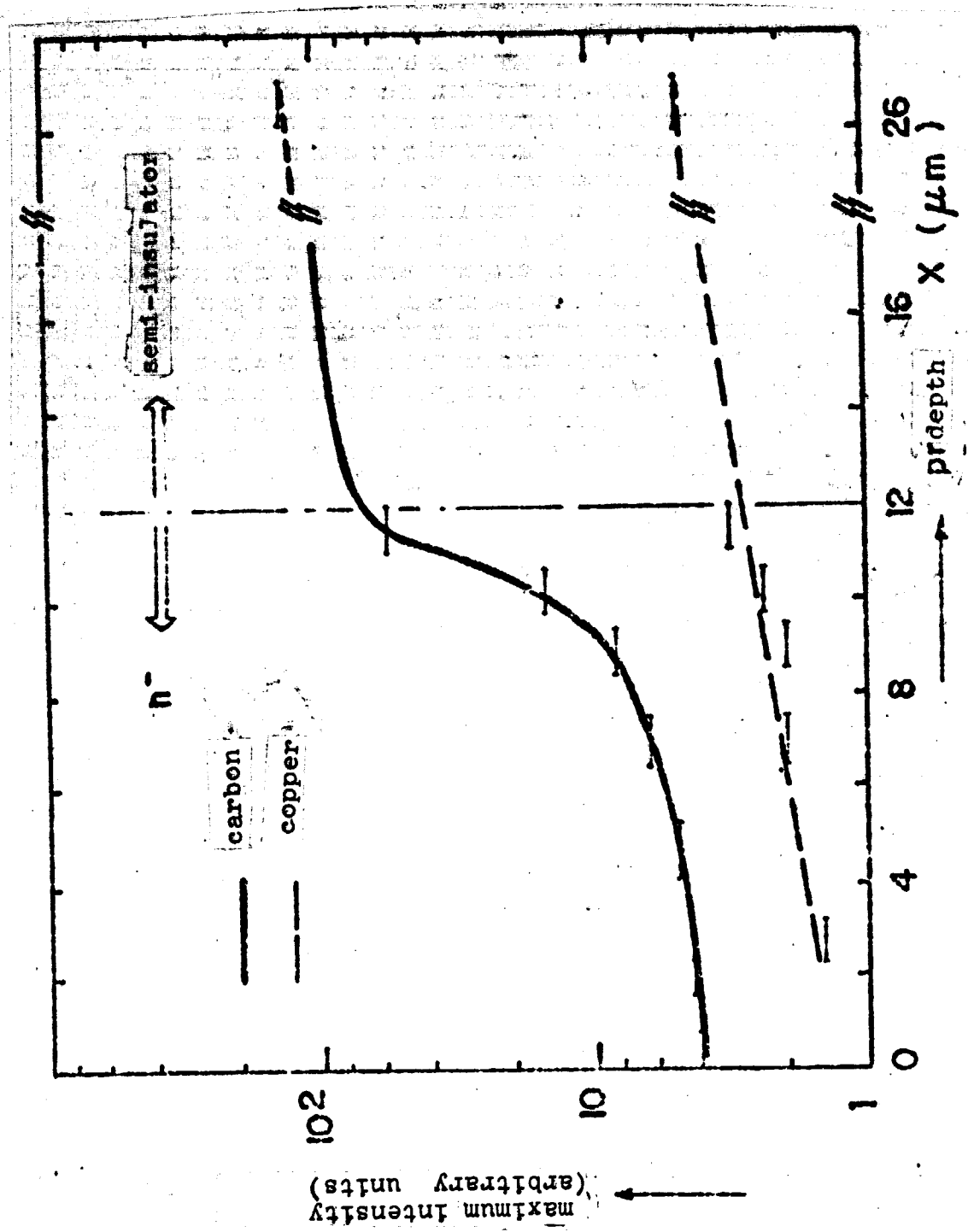
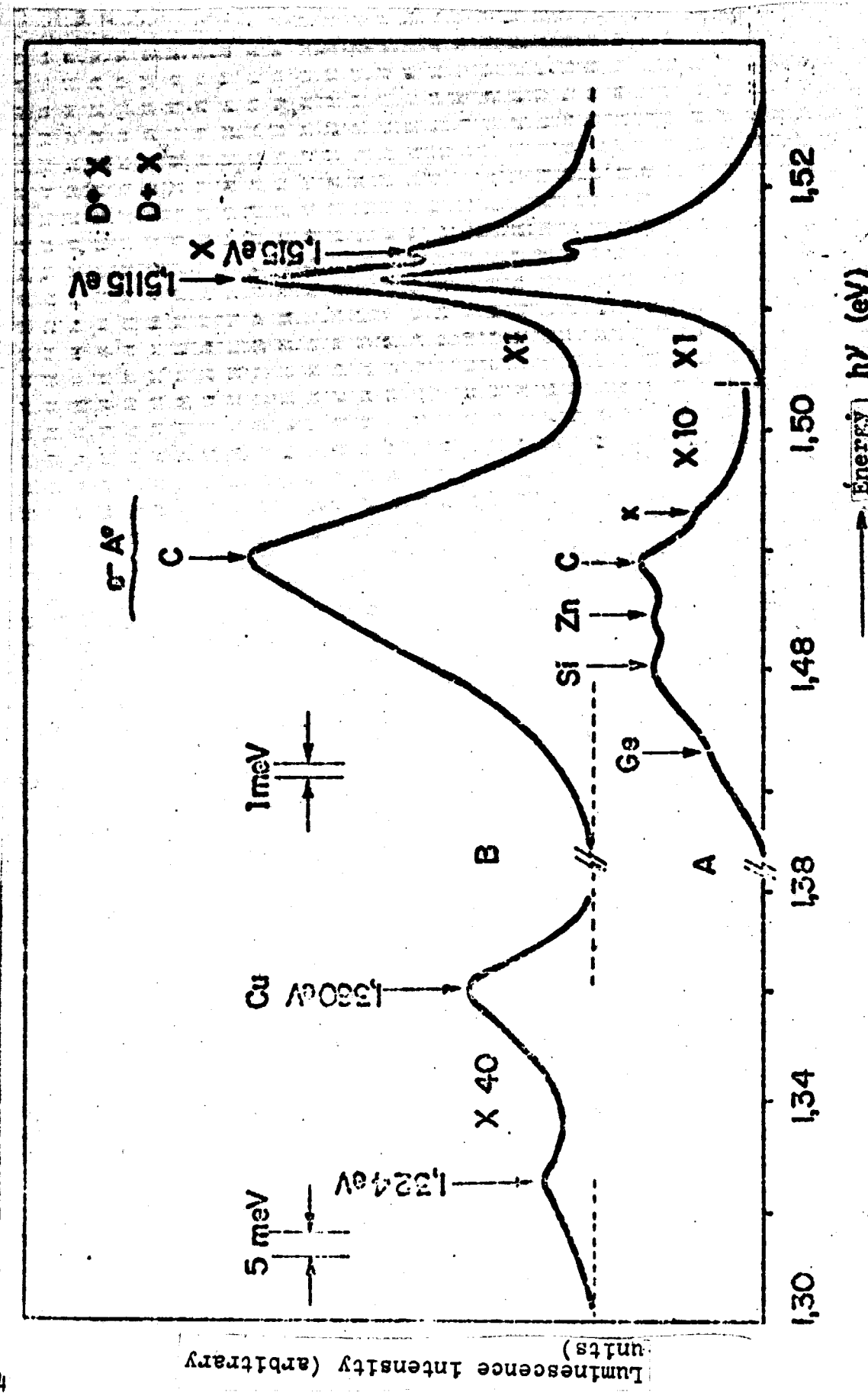


Fig: 12



三  
二  
一

ORIGINAL PAGE IS  
OF POOR QUALITY

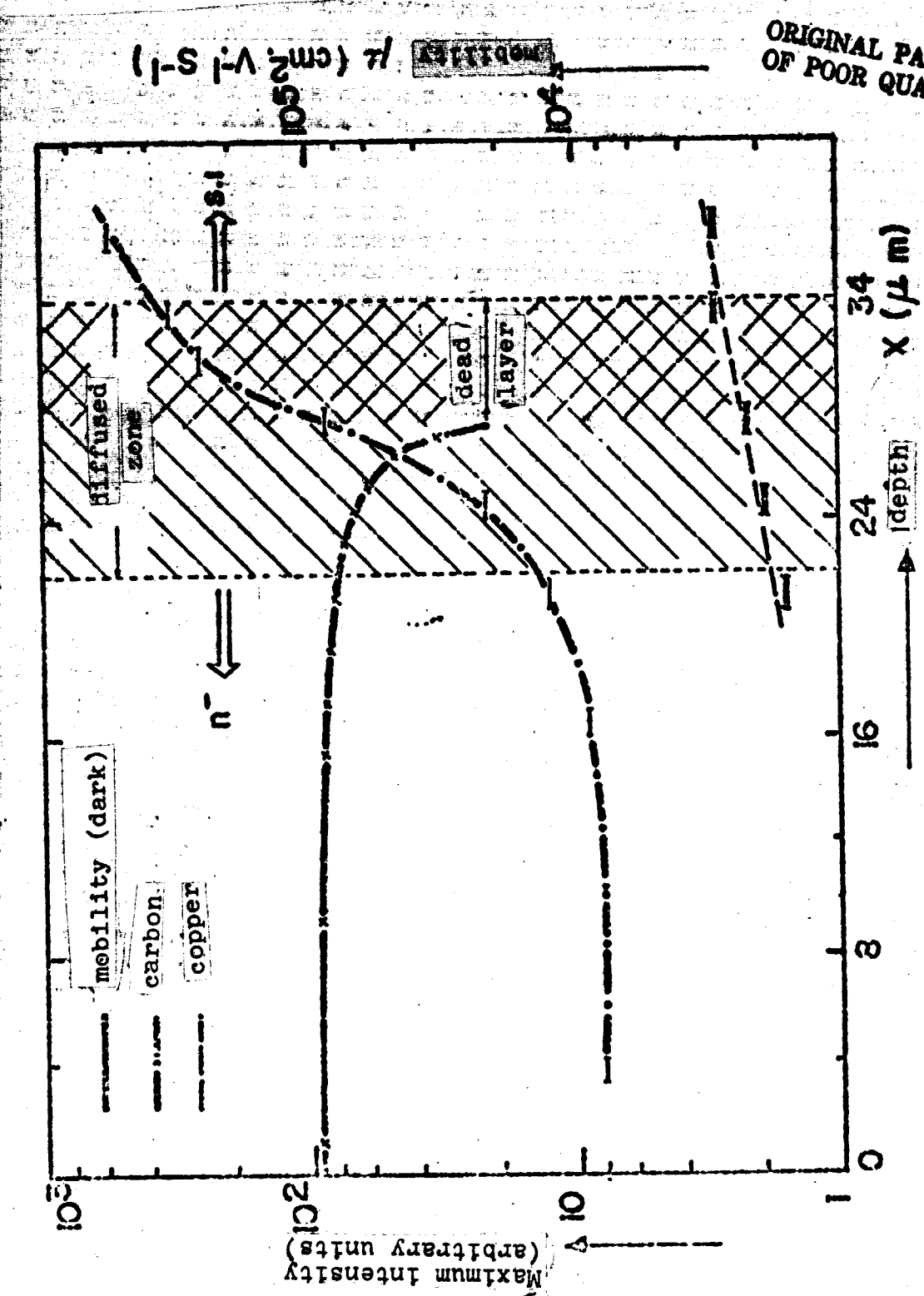
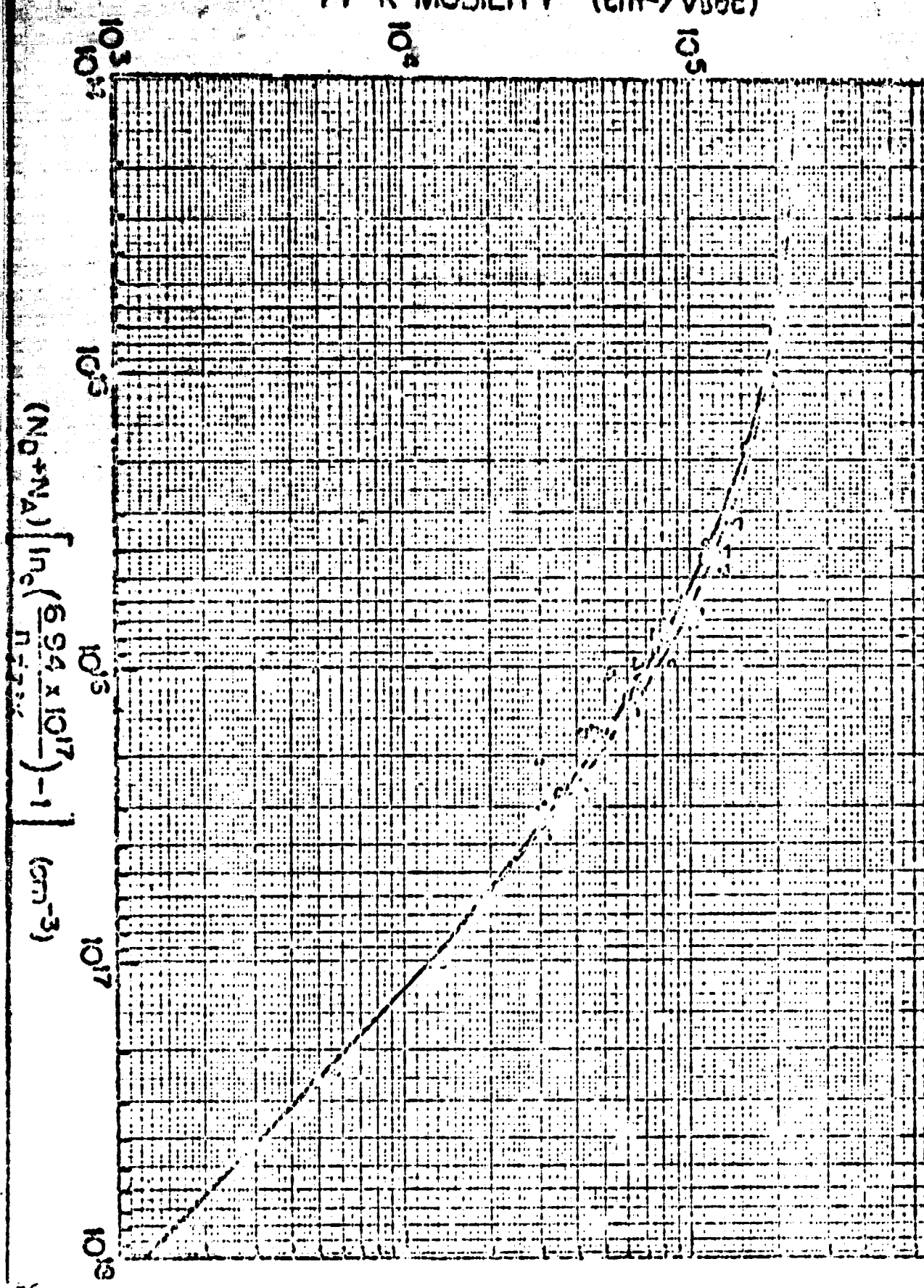


Fig: 14

77°K MOBILITY ( $\text{cm}^2/\text{Vsec}$ )



ORIGINAL PAGE IS  
OF POOR QUALITY

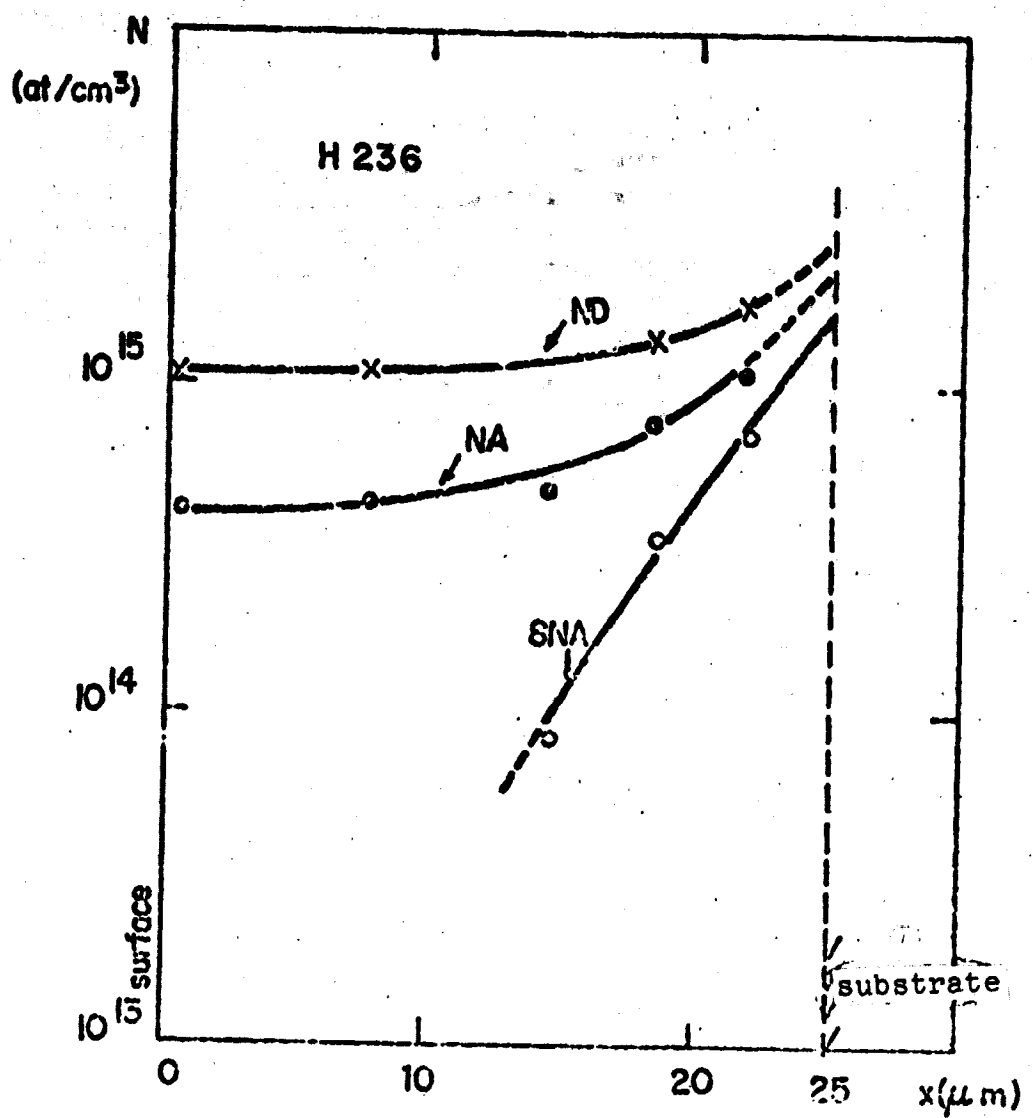


Fig : 16

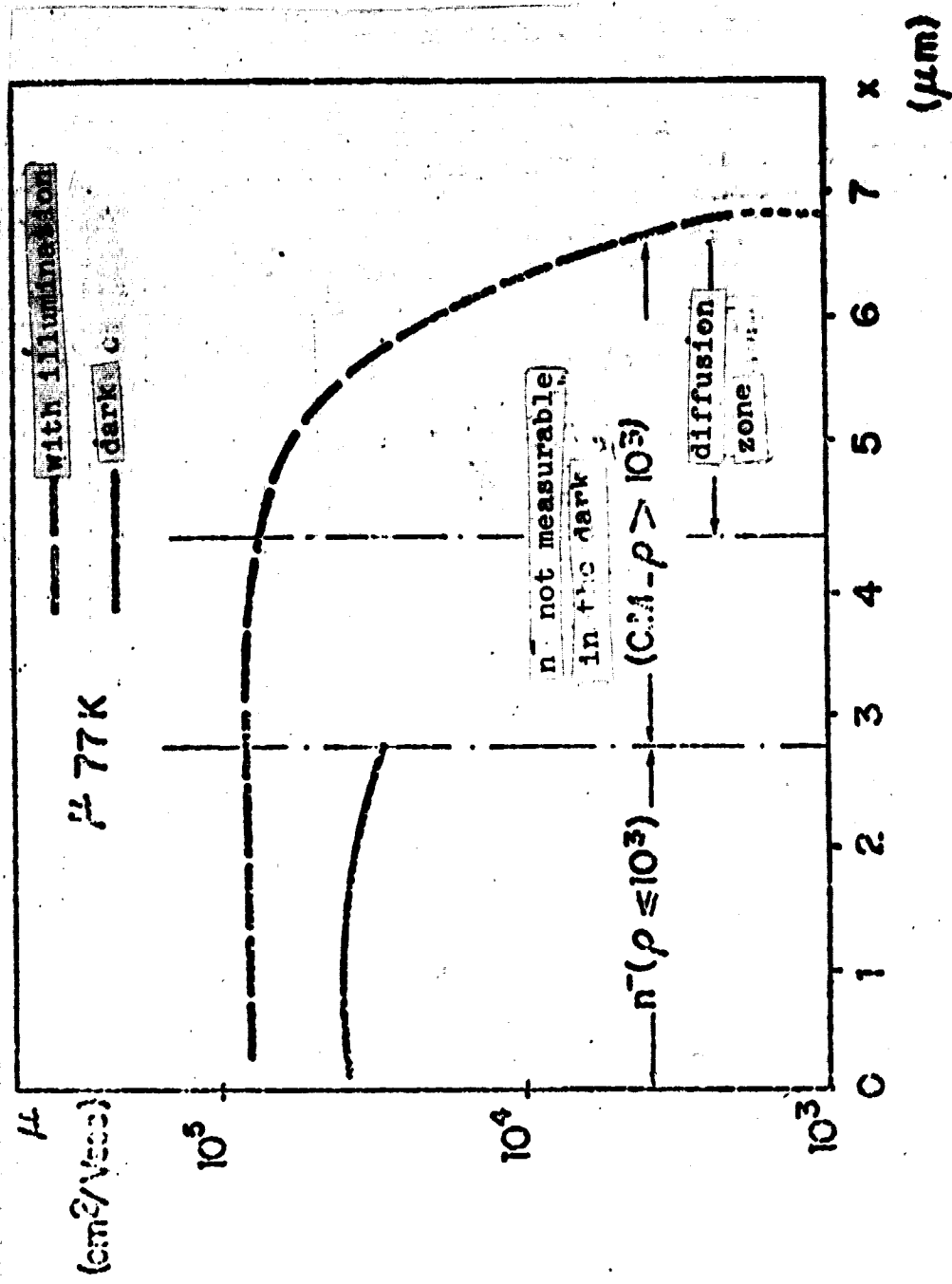


Fig : 17

ORIGINAL PAGE IS  
OF POOR QUALITY

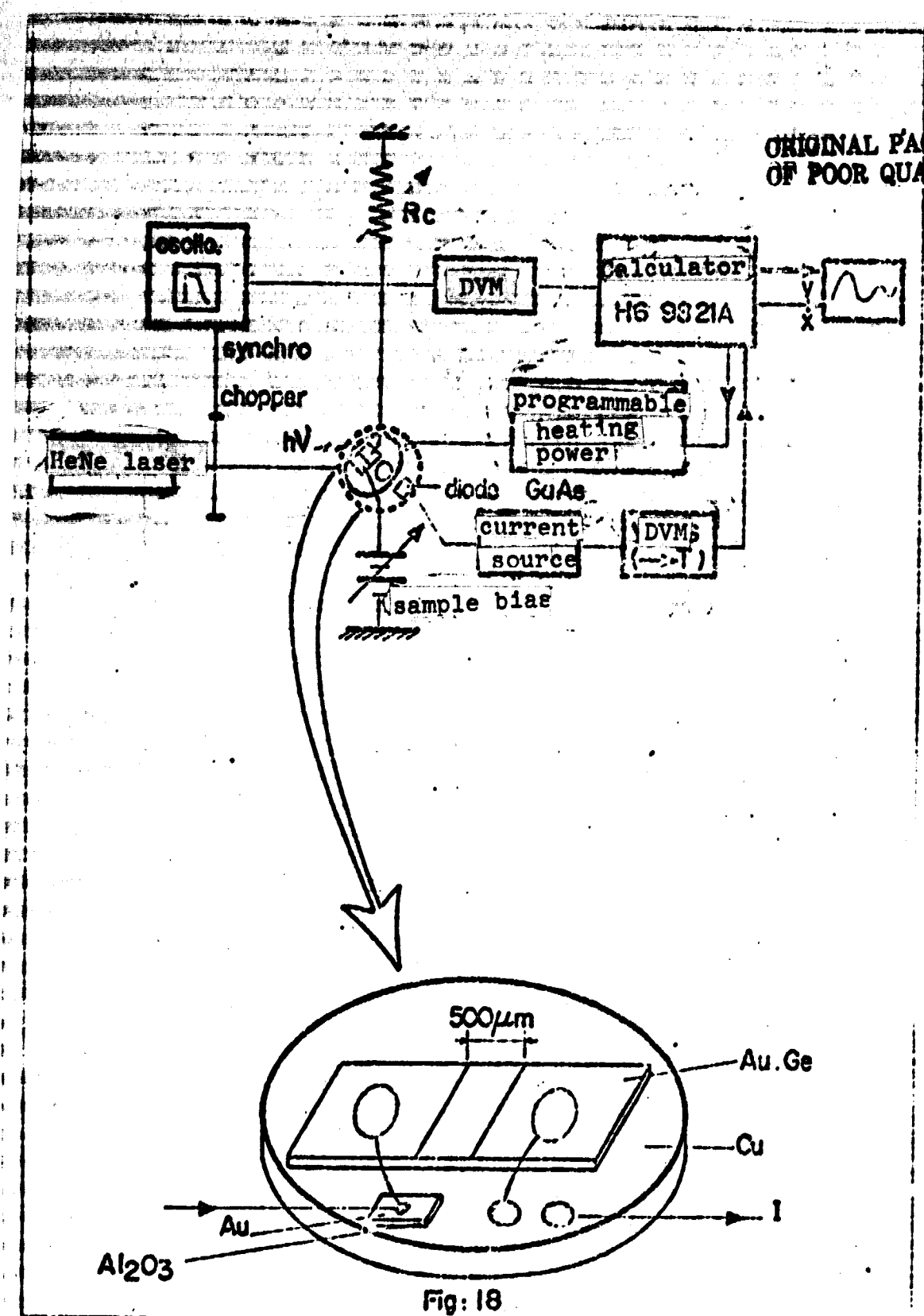


Fig: 18

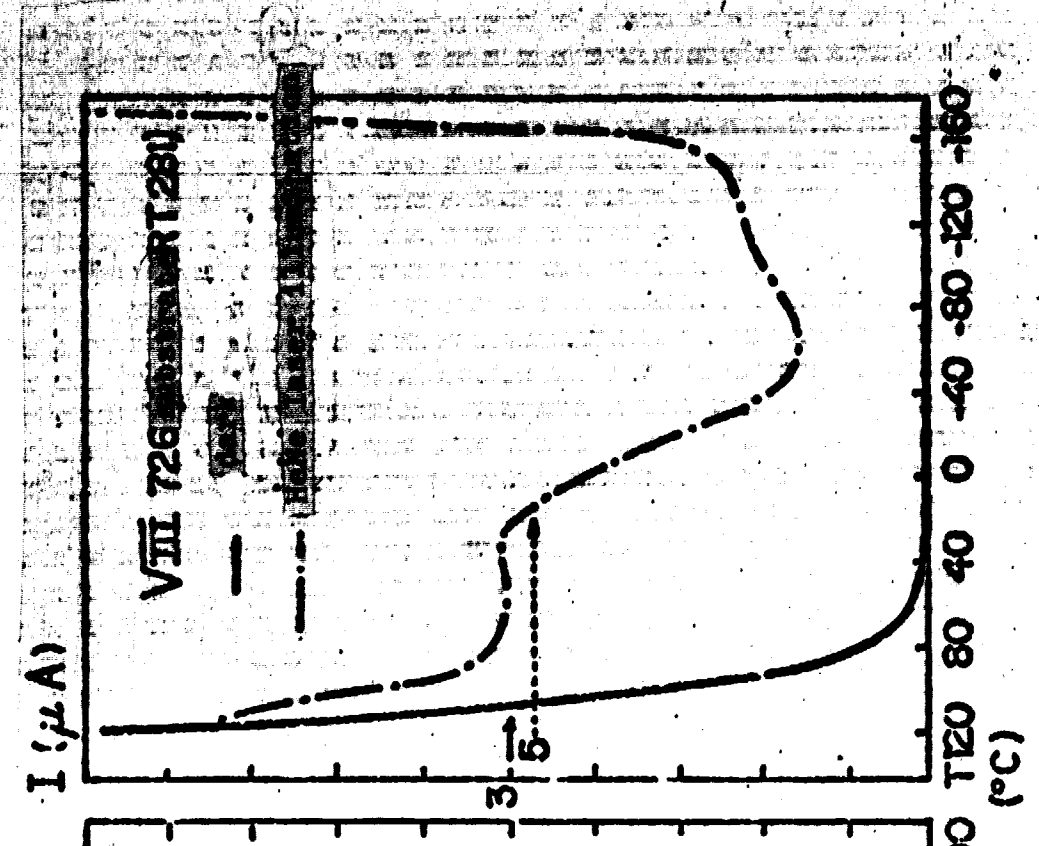
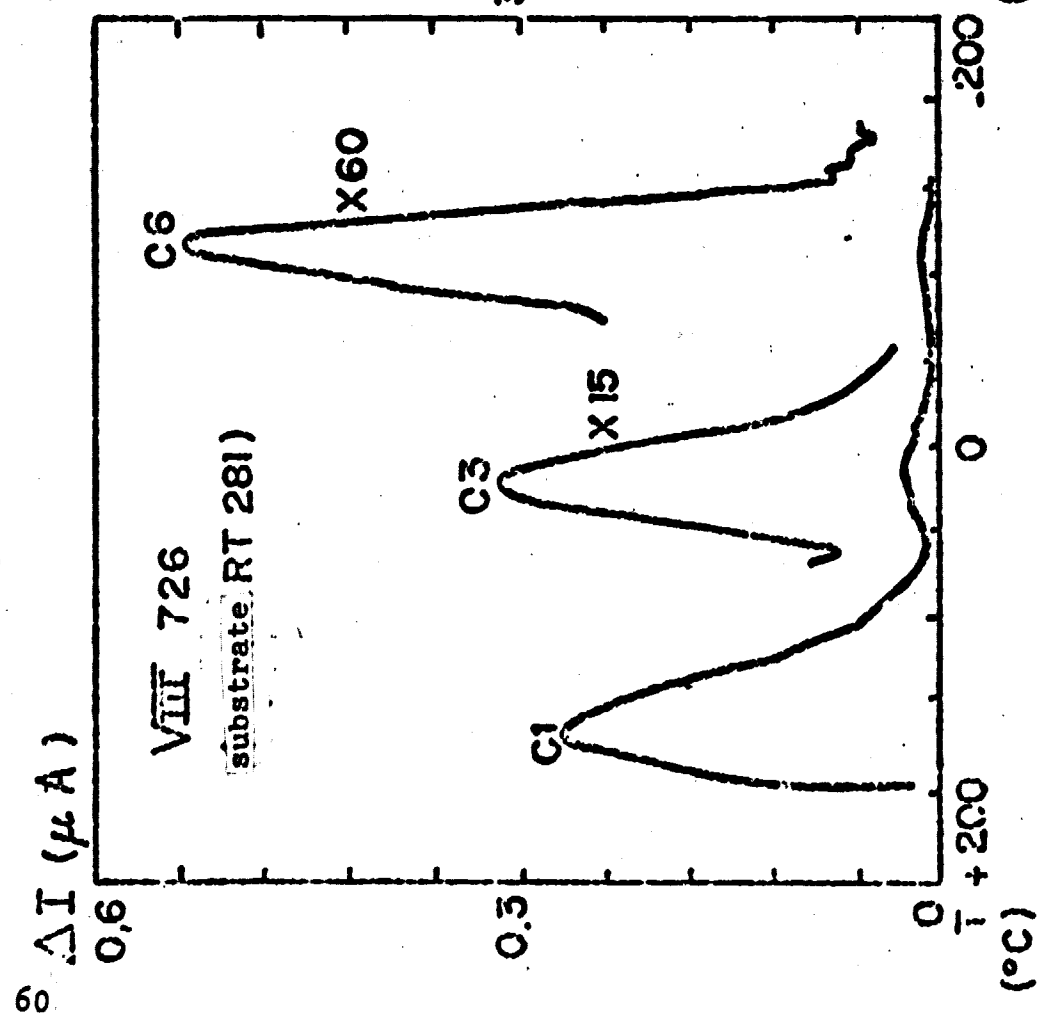


Fig: 19

ORIGINAL PAGE  
OF POOR QUALITY

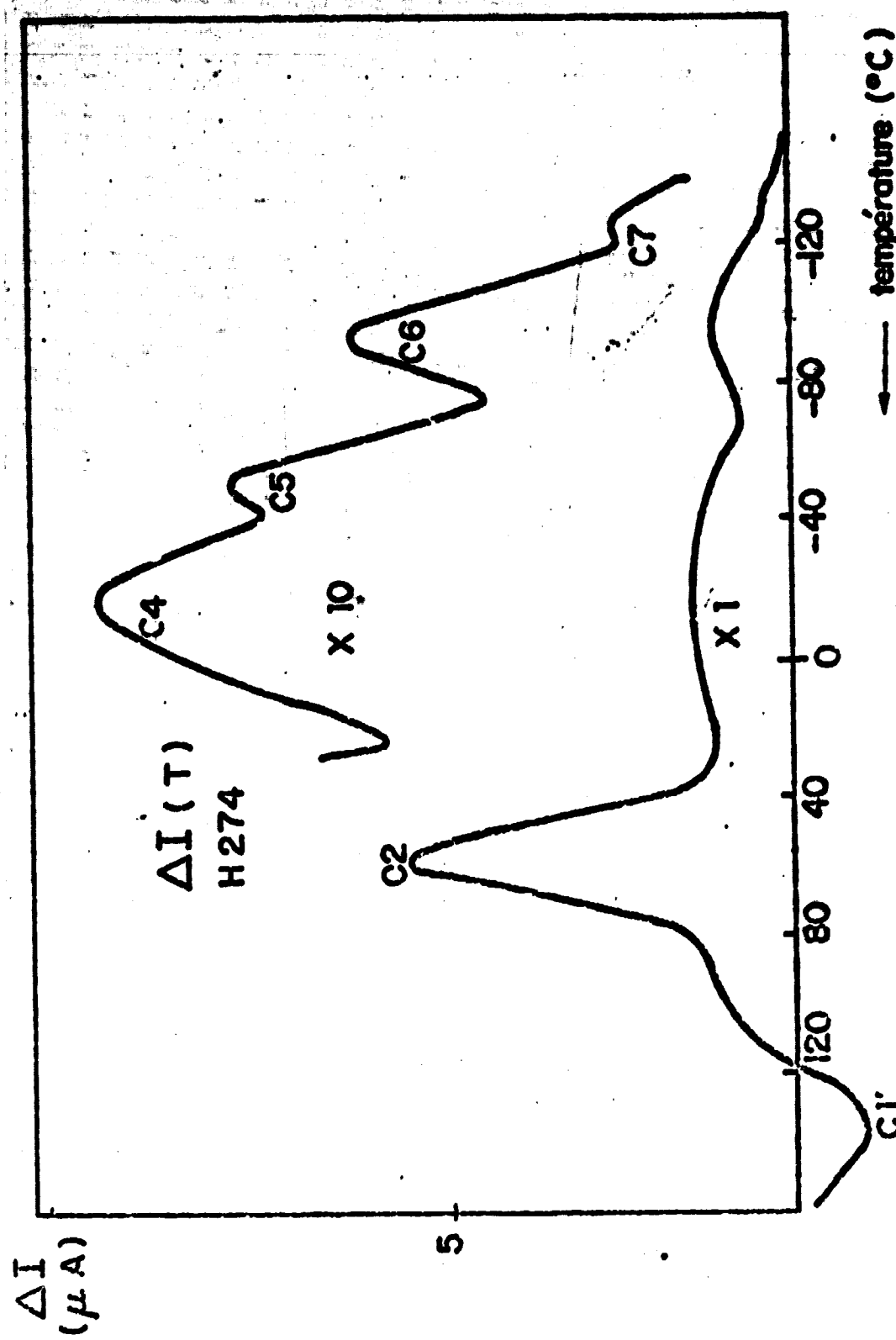


Fig: 20

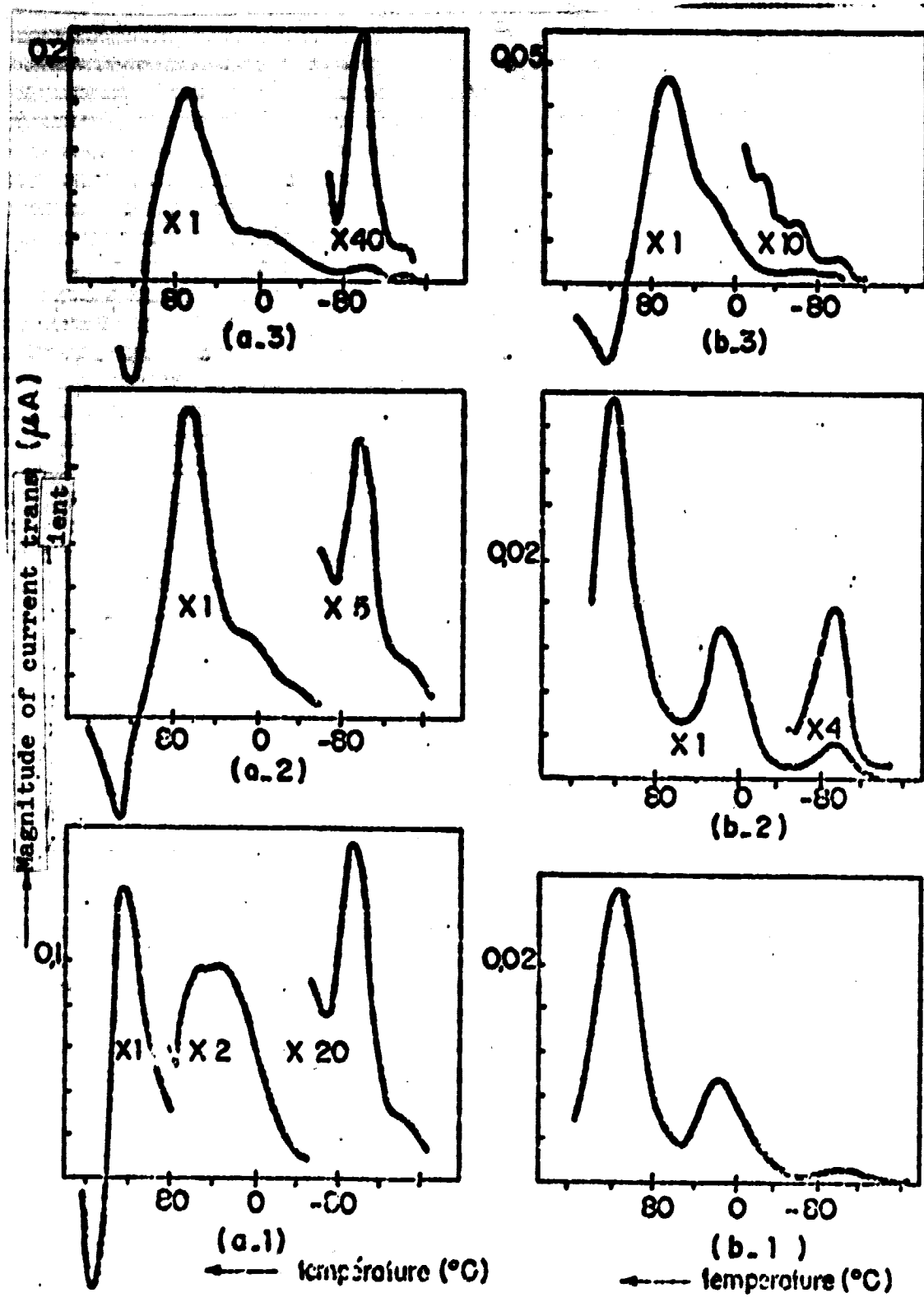
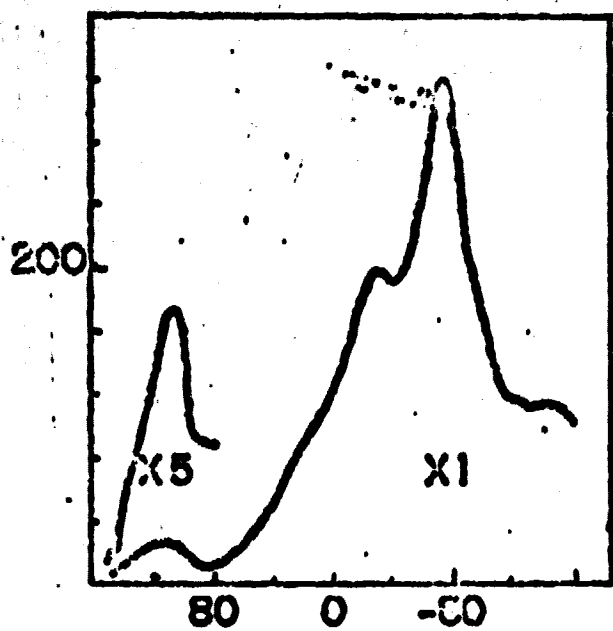
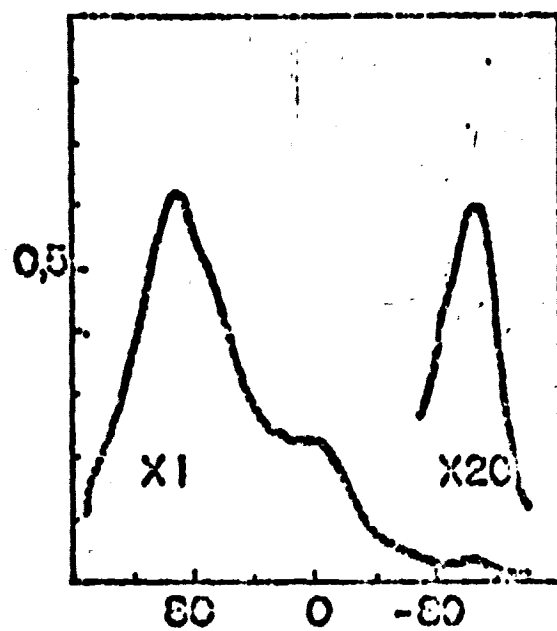


Fig: 21

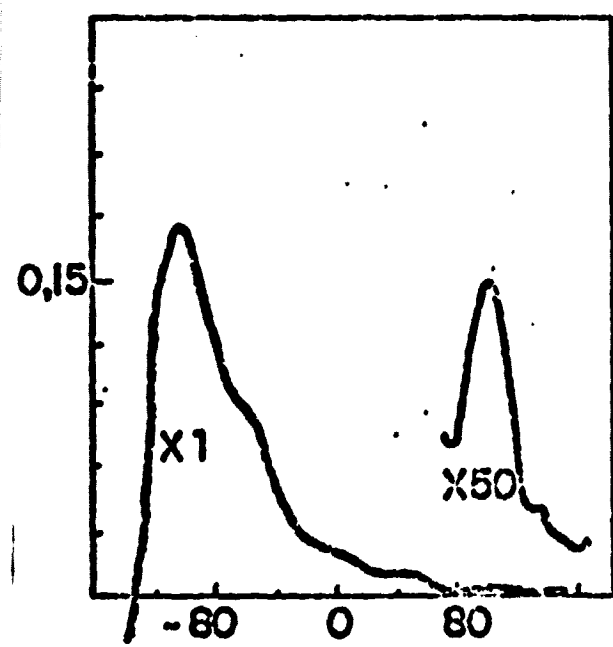
Magnitude of current transient ( $\mu$ A)



- 1 -

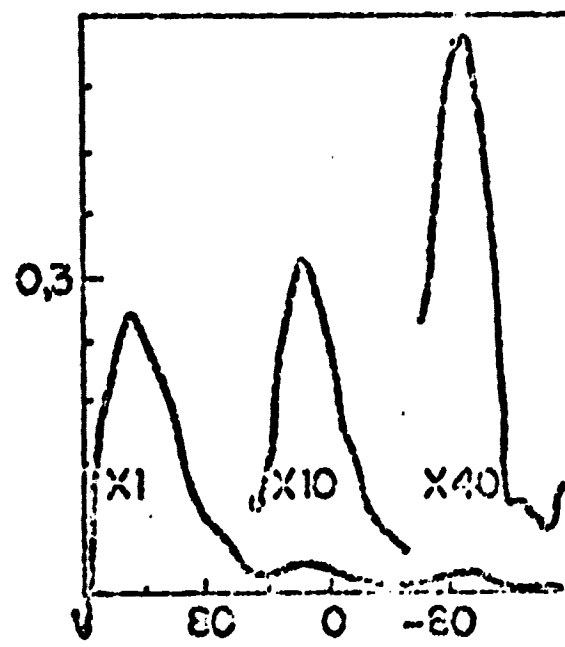


- 2 -



- 3 -

temperature ( $^{\circ}$ C)



- 4 -

temperature ( $^{\circ}$ C)

Fig: 22

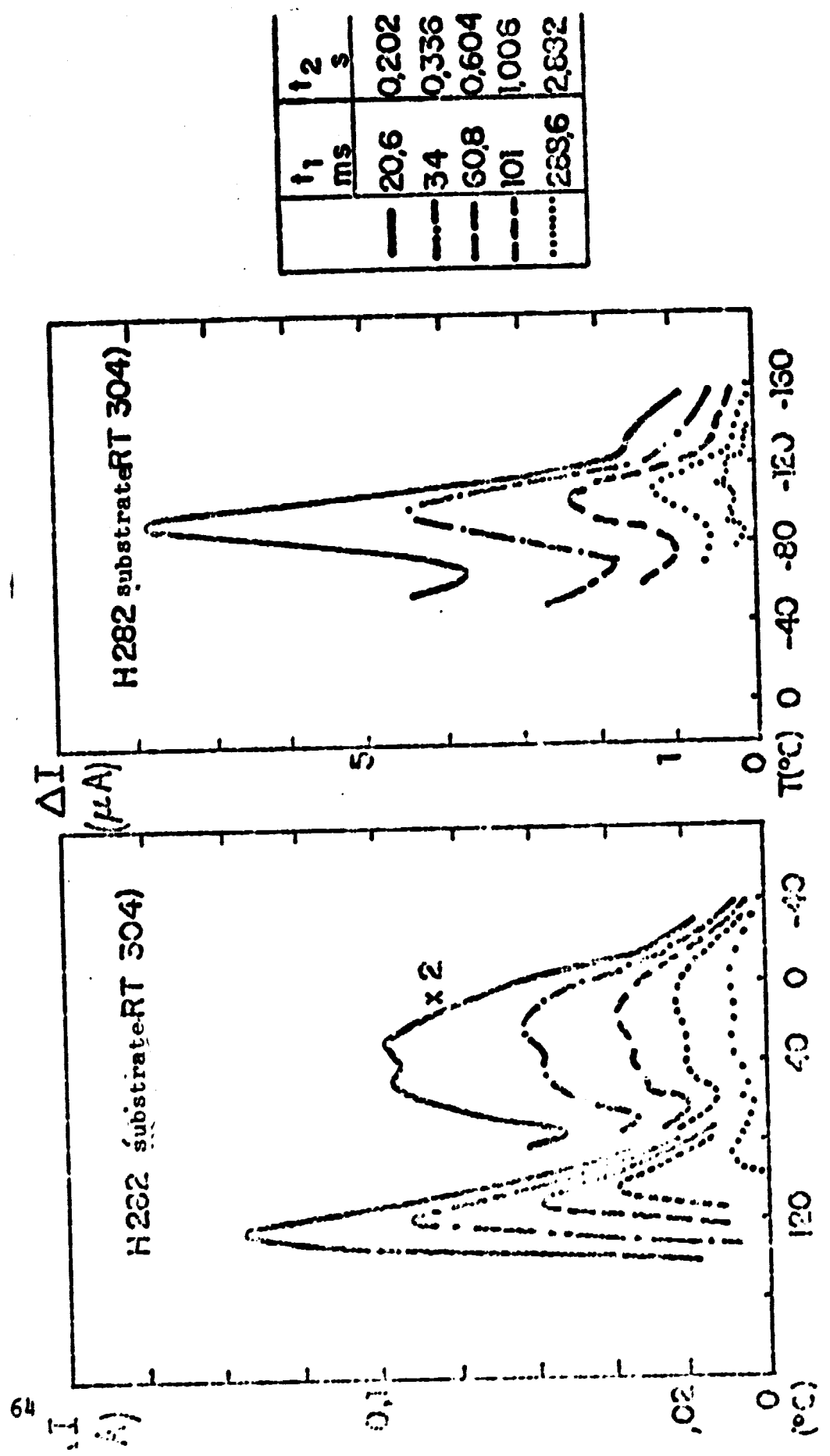


Fig. 25

b)

a)

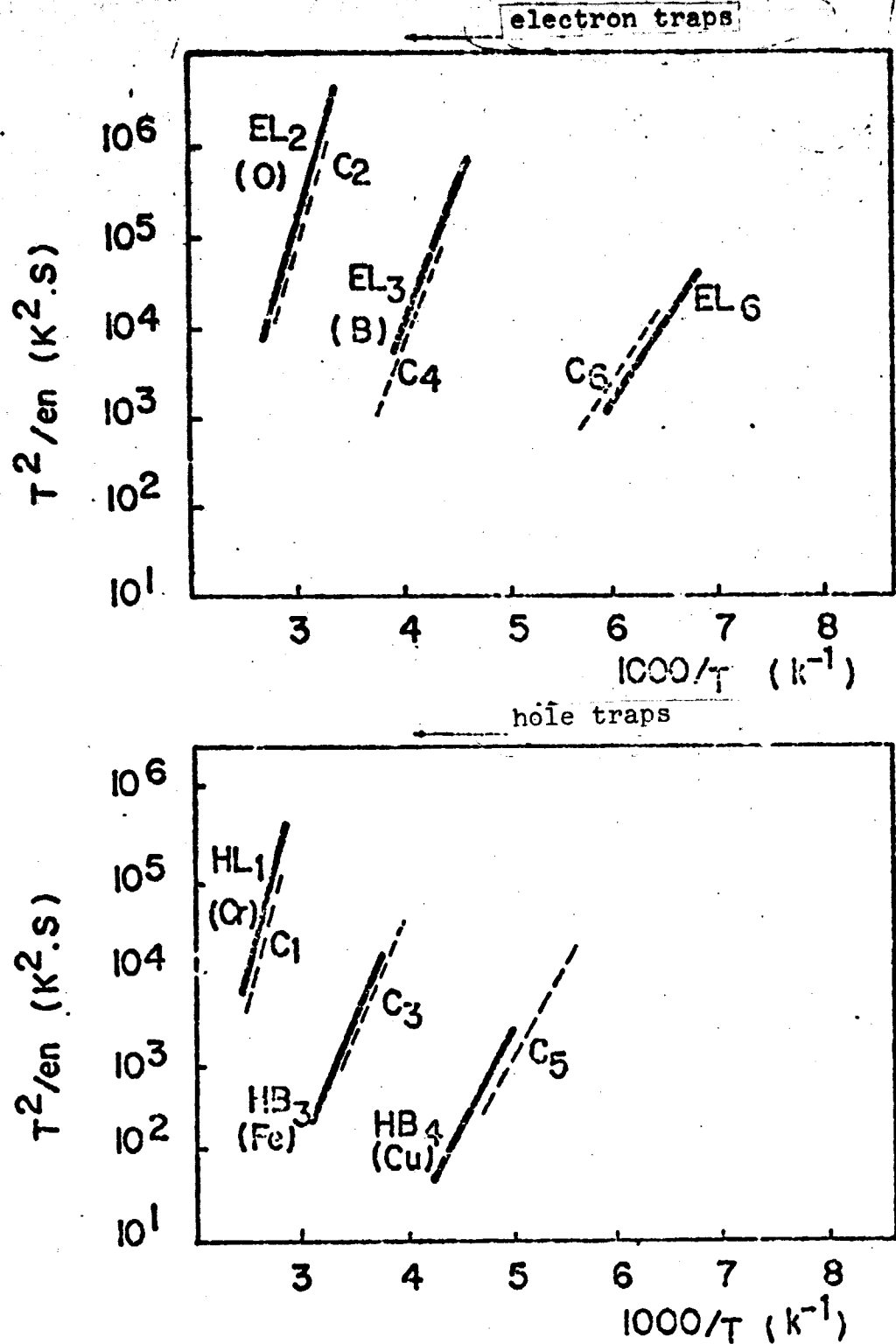


Figure 24

ORIGINAL PAGE IS  
OF POOR QUALITY

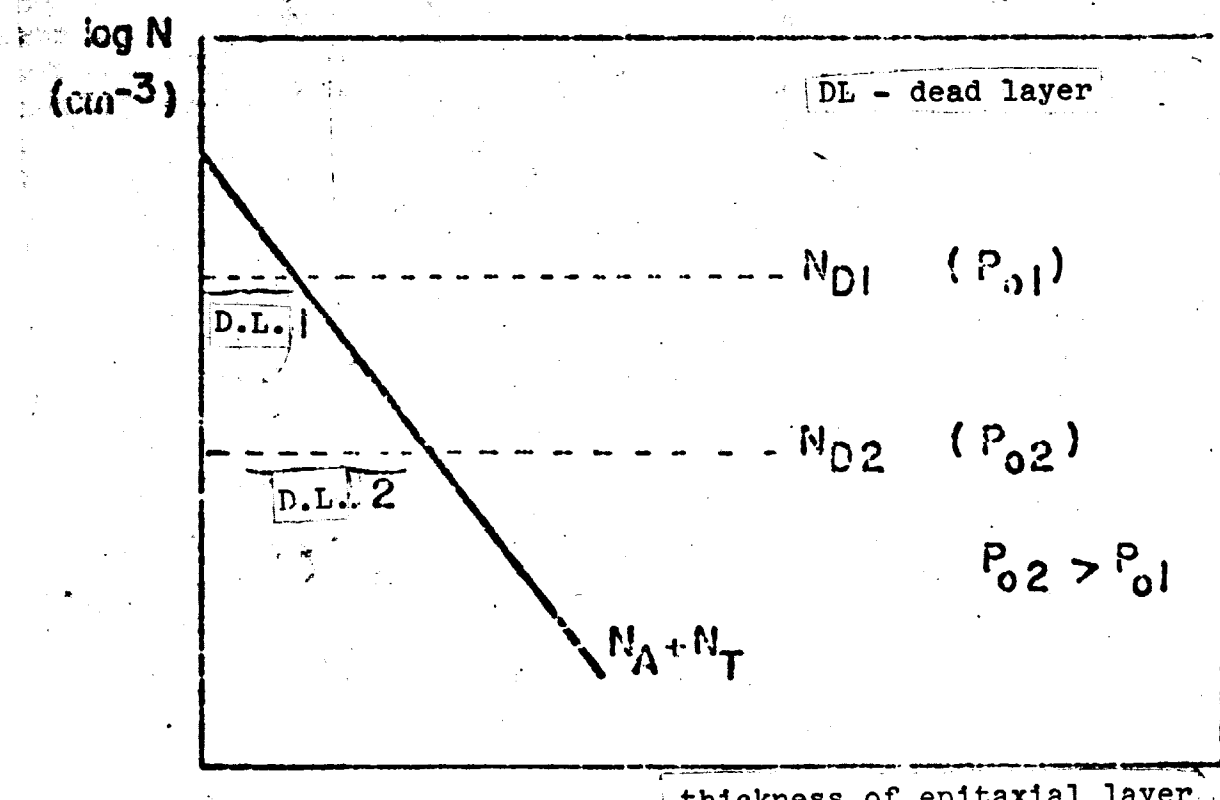
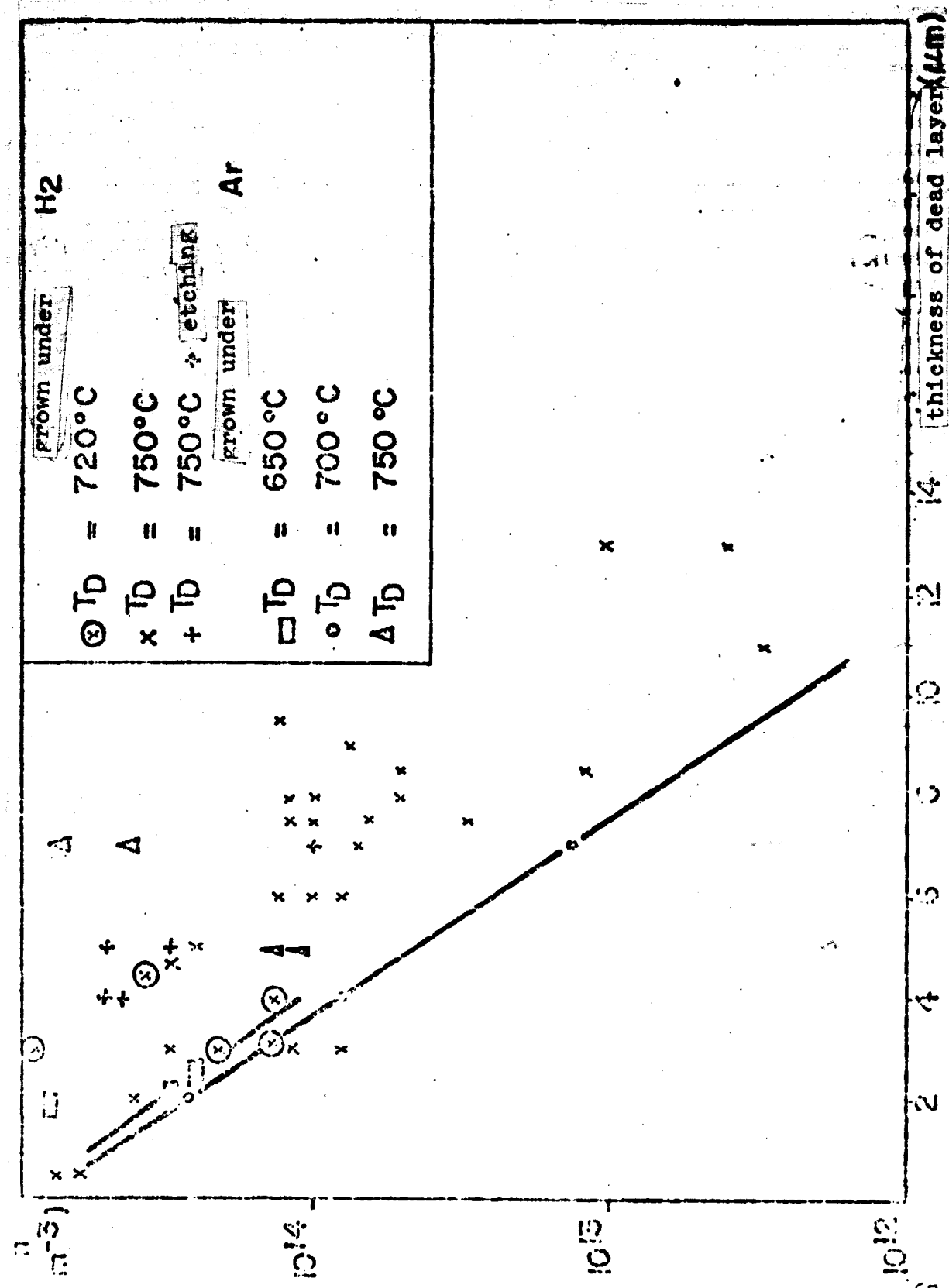
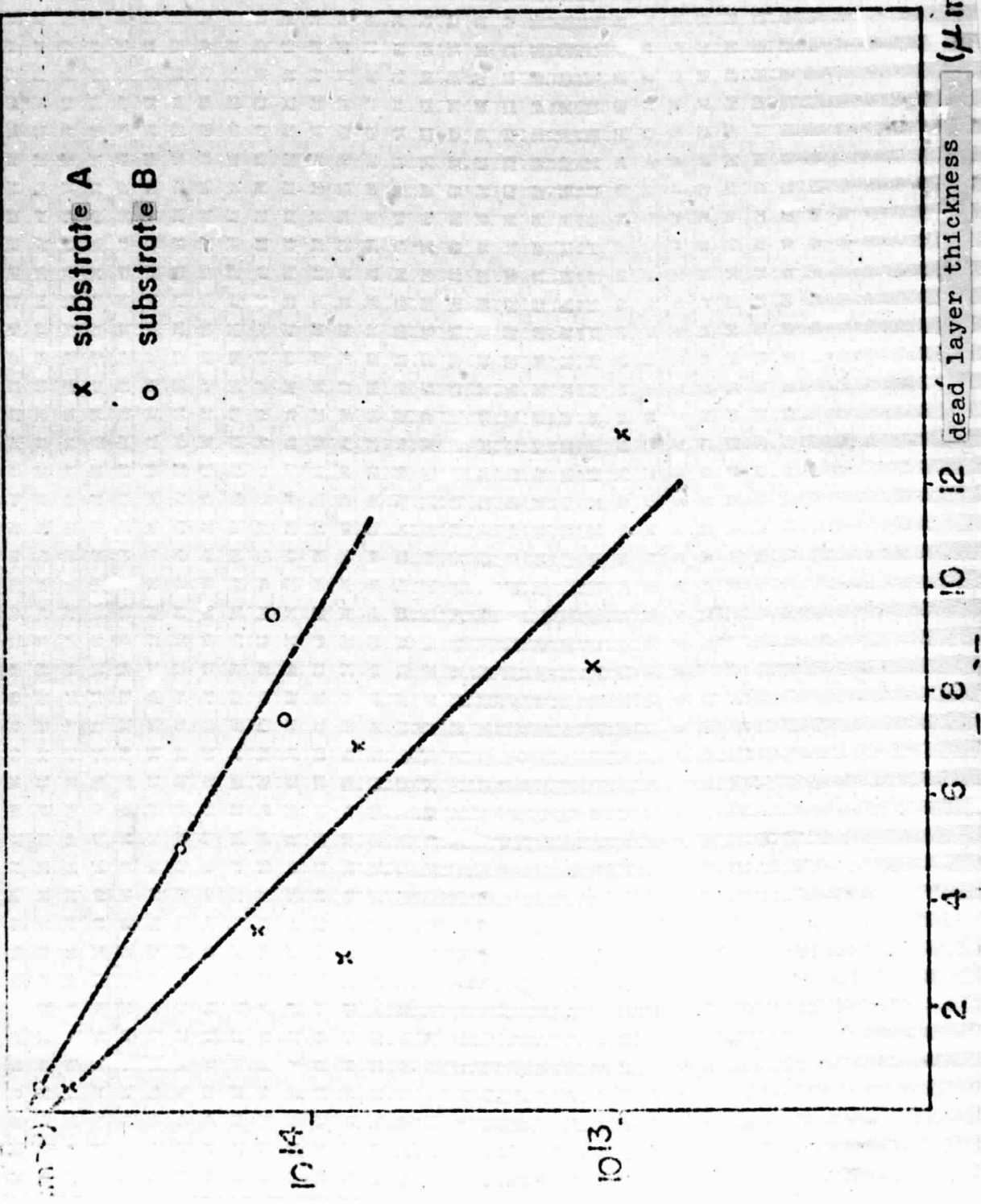


Fig: 25





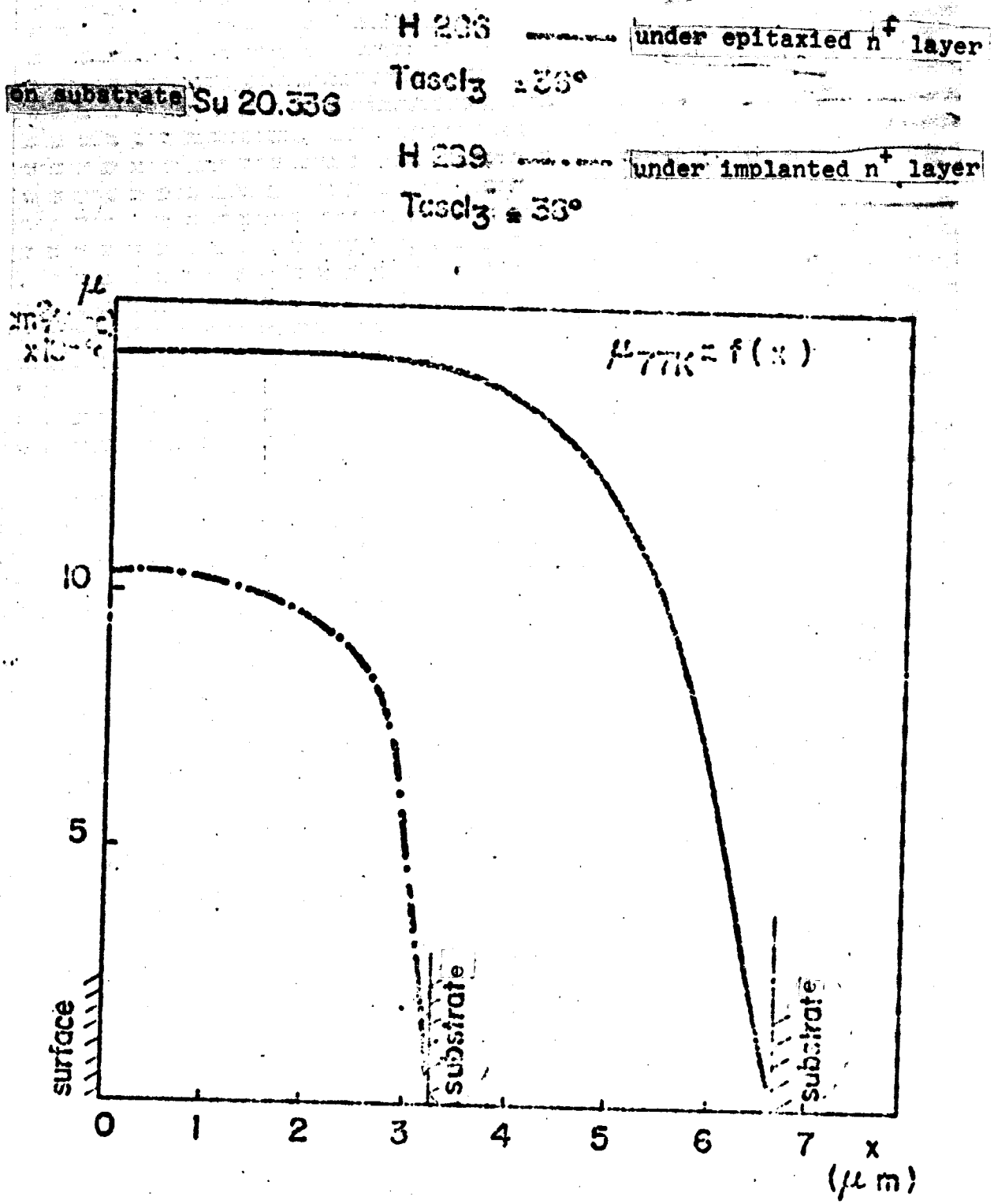


Fig:26

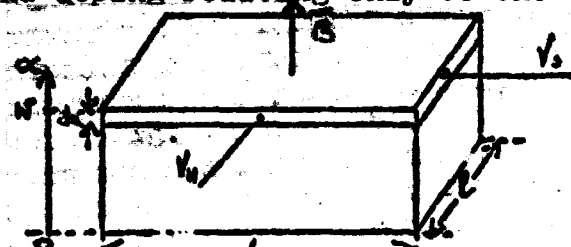
APPENDIX I

Differential calculation of mobilities  
and doping levels in Hall Effect

/74

The sample (lightly doped epitaxial layer in a semi-insulating substrate) is measured by Hall Effect after each etch.

The following calculation allows one to transform the average results over the entire thickness of the remaining layer into values of real mobility and doping relating only to the etched layer.



For the small layer of thickness  $dx$ , the resistivity is written

$$r(x) = \rho(x) \frac{L}{1dx} = \frac{1}{n(x) u(x) e} \cdot \frac{L}{1dx} \quad (1)$$

One injects current  $I$ ; the measured voltage in the absence of the magnetic field is  $V_0$

$$i(x) = \frac{V_0}{r(x)}$$

$$i(x) = \frac{V_0 e 1}{L} n(x) u(x) dx$$

For each sample:

$$I(w) = \int_0^w i(x) = \frac{V_0 e 1}{L} \int_0^w n(x) u(x) dx \quad (I)$$

then  $V_h(x)$ , the Hall voltage measured in the presence of the magnetic field if one only has the little surface layer

$$v_h(x) = \frac{B i(x)}{e n(x) dx} \quad \text{d'où} \quad v_h(x) = \frac{BV_0}{L} u(x) \quad (2)$$

/76

Consider a Hall generator equivalent to our little layer subjected to  $G$ , where  $r'$  is the internal resistance

$$r'(x) = \rho(x) \frac{1}{Ldx} = \frac{1}{n(x) u(x) e} \frac{1}{Ldx} \quad (3)$$

One imagines this generator alone (not distributed) feeding the remainder of the sample of equivalent resistance  $R'$ , where  $V_H$  is the voltage across the edges

$$\frac{1}{R'} = \int_{r(x)}^{\infty} \frac{1}{x} = \frac{BL}{l} \int_0^w n(x) \mu(x) dx \quad (4)$$

Now

$$V_H = v_h \frac{R'}{R' + R}$$

By hypothesis  $r' \gg R'$

so that

$$V_H = V_h \frac{R'}{R'} \text{ d'où } V_H(x) = \frac{BV_0}{L} \frac{n(x) \mu^2(x) dx}{\int_0^w n(x) \mu(x) dx} \quad (5)$$

By superimposing all the generators at the rate of one for each layer of thickness  $dx$ , one obtains the total measured Hall voltage

$$v_H(w) = \int_0^w v_H(x) \quad \text{from which, taking into account of (5)}$$

$$v_H(w) = \frac{BV_0}{L} \frac{\int_0^w n(x) \mu^2(x) dx}{\int_0^w n(x) \mu(x) dx} \quad (\text{II})$$

From the Hall effect one measures  $V_0$ ,  $I$ , and  $V_H$ , from which  $n(x)$  and  $\mu(x)$  can be deduced.

In transforming expressions (I) and (II) and in putting

$$\int_0^w n(x) \mu^2(x) dx = f(w) \quad \text{and } l = L \quad (\text{van de Pauw clover})$$

$$\int_0^w n(x) \mu(x) dx = g(w)$$

where  $f'(w)$  and  $g'(w)$  are the derivatives of these functions.

One obtains finally at one point of the layer of size  $z$

$$\mu(z) = \frac{f'(z)}{g'(z)} \quad \text{and } n(z) = \frac{g'(z)^2}{f'(z)}$$

1. One should write  $r\mu(z)$  and  $n(z)/r$  but we have taken  $r = 1$  for this calculation.
2. for the van de Pauw structure, one can in fact take  $L = 1$  and take account of this for the calculation of the mobility by a multiplicative correction factor  $k = \log 2/\tau$

Appendix TT

/78

**LABORATOIRES D'ELECTRONIQUE ET DE PHYSIQUE APPLIQUÉE**

**3, AVENUE DESCARTES - BP 10  
914450 LIMONNIER-BREVANNES**

**TEL. 560.90.10.**

**CH/DP - 349/78/11**

**January 1978**

**Manuscript for the review :  
Applied Physics Letters**

**DEEP LEVEL SPECTROSCOPY IN HIGH RESISTIVITY MATERIALS\***

**Ch. Marten, M. Boulot, A. Milonniou, D. Bois**  
**Laboratoires d'Electronique et de Physique Appliquée**  
**3, avenue Descartes, 91450 Limonnié-Brevannes (France)**

**Abstract**

A simple method to characterize deep levels in high resistivity materials is described.

Excess carriers are optically injected by pulsed light. The detrapping of these carriers leads to a transient current collected between two contacts. The signal is analysed like in DLTS, i.e. deep level spectra are recorded during temperature cycles. Some examples of the use of this method are given and the calculation of the energy of the levels discussed.

\*This work has been supported by the D.G.R.S.T. (Délégation Générale à la Recherche Scientifique et Technique)

ORIGINAL PAGE IS  
OF POOR QUALITY

### INTRODUCTION

The characterization of high resistivity GaN, either semi-insulating substrates or buffer layers, is now a crucial subject because these materials are used for ion implantation or as substrates for epitaxial growth. This question is of particular interest for FET devices where thin conducting layers are grown on these high resistivity materials.

Powerful techniques have been recently developed to improve the classical methods of deep level characterization in semiconductors<sup>1)</sup>: transient capacitance measurements such as DLTS<sup>2)</sup> and optical DLTS<sup>3)</sup>, or transient current analysis with diode structures<sup>4, 5)</sup>. These techniques fail for high resistivity materials.

It is the purpose of this paper to report about a simple method for deep level characterization in high resistivity semiconductors.

### EXPERIMENTAL TECHNIQUES

In high resistivity materials, carriers cannot be easily injected by electrical means. So, in the proposed method, they are optically generated in the material. Then, detrapping is monitored versus temperature by transient current measurements.

Figure 1 shows the block diagram of the experiment. Electron-hole pairs can be generated by using a He-Ne laser ( $6328 \text{ \AA}$  - 5 mW) or a GaN electroluminescent diode ; at low temperature, photocarriers are then captured by respectively electron or hole traps. After the optical injection pulse (duration 30 ns), detrapping creates a transient current between the two contacts evaporated onto the sample surface.

The dark equilibrium current :  $i_{\infty}$ , the photoconductive current  $i_{ph}$  (during illumination), and the transient current are measured. A single gate technique could be used<sup>6)</sup>. However in the

ORIGINAL PAGE IS  
OF POOR QUALITY

high temperature range  $i_{ph}$  is non negligible so a double gate technique was more suitable :  $i(t_1) - i(t_2)$  is measured with  $t_2 \gg t_1$ , so that  $i(t_2) \approx i_{ph}$ . This signal analysis is identical to the one in classical DLTS, so the same apparatus can be used. The system we use has been described previously<sup>7</sup>. It includes a calculator which stores the data and controls the process : temperature changes, injection pulses, applied voltage.

According to Lang's technique, a simple temperature cycle (between 77 K and 500 K in this particular case) provides a deep level spectrum. Figure 3 shows typical spectra obtained with high resistivity ( $\rho \geq 10^3$  ohms.cm) buffer layers prepared by vapor phase epitaxy.

#### CALCULATIONS

At  $t = 0$ , at the beginning of the transient, after an intrinsic excitation (e-h generation), the occupancy of a particular trap with, for instance, two charge states (+, 0) is :

$$N_T^0(0) = \frac{N_T}{1 + \frac{\epsilon_n \cdot G_p v_p \delta_p}{\epsilon_p \cdot G_n v_n \delta_n}} \quad (1)$$

where  $N_T$  is the density of traps,  $\epsilon_n$  and  $\epsilon_p$  the sum of the thermal and optical emission rates for e- and h+ respectively,  $G_n$ ,  $G_p$ ,  $v_n$  and  $v_p$ , the corresponding capture cross sections, and thermal velocities, and  $\delta_n$ ,  $\delta_p$ , the densities of injected carriers during illumination. They are assumed to be large compared to the dark carrier densities. This can be verified by looking at the ratio  $i_{ph}/i_{ph}$  which is generally high.

At  $t \rightarrow \infty$ , the dark equilibrium is described by :

$$N_T^0(\infty) = \frac{N_T}{1 + \frac{e_n}{e_p}} \quad (2)$$

The free carrier densities are assumed to be negligible in the high resistivity materials considered in this work.

The current generated by this trap is (1) :

$$I(t) = C [e_n N_T^0(t) + e_p (N_T - N_T^0(t))]$$

The constant C includes the geometrical parameters and the penetration depth of the light. The transient current  $\delta I(t)$  which is of interest in the double gate technique can be written :

$$\begin{aligned} \delta I(t) &= [I(0) - I(\infty)] \exp. - \frac{t}{\tau} \\ \text{i.e. } \delta I(t) &= C (e_n - e_p) [N_T^0(0) - N_T^0(\infty)] \exp. - \frac{t}{\tau} \end{aligned} \quad (3)$$

$$\text{with } \frac{1}{\tau} = (e_n + e_p).$$

In order to simplify the discussion, we have to distinguish between several cases.

### (i) trap with $e_n \gg e_p$

Under conditions of high excitation,  $e_n$  and  $e_p$  can be neglected compared to  $G_p v \delta n$  and  $G_n v \delta n$ , then (3) together with (2) and (1) gives :

$$\delta I(t) = C e_n N_T \left[ \frac{1}{1 + \frac{G_p v_p}{G_n v_n}} - \frac{1}{1 + \frac{e_n}{e_p}} \right] \exp. (-e_n t) \quad (4)$$

which is independent of the excitation flux.

A more complicated formula is obtained under lower excitation. The corresponding transient current depends on the excitation intensity. Therefore, the high excitation condition can be experimentally checked by varying the intensity and looking for saturation; obviously, this is easier to satisfy for small emission rates, i.e. w rather large values of  $t_1$  are chosen. In the following, we suppose the high excitation is achieved.

for  $\tau_n/\tau_p \gg 1$  (electron trap) the preceding formula reduces

$$S(t) = C N_T e_n \exp(-\alpha_n t) \quad (5)$$

which is the simple classical formula for the transient current due to emptying of a trap completely refilled at  $t = 0$  and emptied at  $t_{\infty}$ .

By derivation of (5) with respect to temperature for a fixed delay  $t_1$ , one finds that a maximum occurs when :

$$\frac{1}{t_1} = \alpha_n (T_{\max}) = \tau_n v_n N_e \exp(-\frac{E_T}{kT_{\max}}) \quad (6)$$

where  $T_{\max}$  is the temperature corresponding to the maximum of  $S(t)$ , and  $E_T$  the energy of the trap below the conduction band.

Under such conditions, the energies of the levels can be easily found by running spectra with different sampling delays  $t_1$  like in classical DLTS measurements. This is illustrated in fig. 3 for the shallower trap of figure 2. The delays are always chosen with  $t_2 = 10 t_1$ . The plot  $T^2/\alpha_n$  versus  $1/T$  (insert of fig. 3) provides :  $E_T = 0.32 \text{ eV} \pm 0.03 \text{ eV}$ . A similar curve, obtained through DLTS, for trap EL 6 of ref. 8 detected in conductive GaAs has been plotted for comparison. It turns out that this defect we observe in V.P.E. buffer layer on Si substrate can be considered as identical to EL 6 of ref. 8 :

- for  $\tau_n/\tau_p \lesssim 1$ , relation (4) does not reduce to (5) : the pre-exponential factor is divided by  $(1 + \frac{\tau_p v_p}{\tau_n v_n})$ . This may change the temperature at which the maximum occurs because  $\tau_p$  and  $\tau_n$  may depend on temperature.

However, this shift of the peak is not very large because the factor  $\exp(-\alpha_n t)$  is predominant.

A similar discussion can be carried out for  $v_p \gg v_n$  : therefore, the characteristics of all the deep levels (provided that one emission rate is large compared to the other) can be determined by using relation (6) and several delays  $t_1$ . This has been done for the traps visible in fig. 2. The energies so found are written down in the figure.

(iii)  $e_n > e_p$

This may arise for traps located near the middle of the gap, for instance chromium and "oxygen" in GaAs<sup>9)</sup>. The time constant in (3) is then  $\frac{1}{Z} \approx (e_n + e_p)$ . It is therefore impossible to determine separately the ionisation energies  $E_n$  and  $E_p$  relative to CB and VB respectively. The situation is indeed identical in capacitive DLTS : even if one type of carrier is injected, the time constant for reemission may be related not only to the emission rate for these carriers but also for the opposite type of carriers. This may lead to some uncertainty in the results for level located near the middle of the gap.

Moreover, in this case, the transient current may be negative as visible in relation (5) if the following condition is fulfilled :

$$\frac{\tau_n}{\tau_p} < \frac{e_p}{e_n}$$

This probably explains the negative peak which appears in some sample at high temperature as shown for one sample in figure 2. According to the calculations, negative transient currents can also arise when  $e_n \gg e_p$  provided the preceding condition is satisfied.

CONCLUSION

The optical transient current spectroscopy, described in this paper, appears to be a very useful method for characterizing high resistivity materials. It gives deep level spectra exactly as classical DLTS does for conducting samples. The spectra directly provide the emission rates of the deep levels, therefore it is very easy to determine the ionisation energies of each level. This is a major advantage compared to TSC which is often used for high resistivity materials. Four deep levels have generally been found using this technique in our epitaxial buffer layers : 0,9 eV, 0,8 eV, 0,58 eV, 0,32 eV, ( $\pm 0,03$  eV).

As discussed in the previous section, the higher is the excitation intensity, the more insulating the material, the more different the emission rates and capture cross sections for electron and holes, the better is the accuracy of the energy value

The main limitations are that it is difficult to calculate the concentration of the traps in a simple way and that as far as now, we cannot be sure whether  $E_t$  is measured with respect to the valence or conduction band.

Beside the identification of deep levels in semi-insulating materials, a very interesting application of this optical transient current spectroscopy is the determination of deep level profiles in strongly compensated buffer layers deposited on semi-insulating substrates. This is possible by using intrinsic excitation which injects carriers in a thin layer below the surface only. Then, by successive chemical etching of the sample, one gets a profile with a spatial resolution limited mainly by the carrier diffusion length. Such study is being carried out and will bring useful information about the defects and impurities introduced by the semi-insulating substrates in the epitaxial layer.

#### Acknowledgements

The authors are indebted to A. Mircea and G.M. Martin for fruitful discussions.

### Bibliography

1. C. T. Sah, L. Forbes, L. L. Rosier and A. F. Tasch  
Solid State Electron, 13, 759, (1970).
2. D. V. Lang, P.A.P., 45, 3023 (1974).
3. A. Mitonneau, G. M. Martin, A. Mircea  
Elect. Lett., 13, 666, (1977).
4. B. W. Wessels  
J.A.P., 47, 1131, (1976)
5. J.C. Brabant, F. Voillot-St-Yves, G. Vassal, M. Brousseau  
Communication a l'ESSDERC (Brighton 1977)
6. D. Bois, J. Phys. (f), 35, C3 - 241, (1974).
7. A. Mitonneau, Phil. Res. Rep. 31, 244, (1976).
8. G. M. Martin, A. Mitonneau, A. Mircea, Elect. Lett., 13, 191,  
(1977).
9. D. V. Lang, R. A. Logan, J. Elect. Mat., 4, 1053, (1975).

Figure Captions

**Fig. 1.** Principles of the experiment

**Fig. 2.** Typical deep level spectrum:  $i(t_1) - i(t_2) = f(T)$  for two GaAs VPE buffer layers grown on a semi-insulating substrate

$$t_1 = 60.8 \text{ ms}$$

$$t_2 = 10t_1$$

**Fig. 3.** Influence of the delay  $t_1$  on a particular peak of figure  
The insert shows the variation of

$$\frac{T^2}{e_n} \text{ versus } \frac{1}{T}$$

obtained with this work (solid line).

The dotted line is for trap EL 6 of ref. 8 (classical DLTS on a GaAs conducting sample).

ORIGINAL PAGE IS  
OF POOR QUALITY

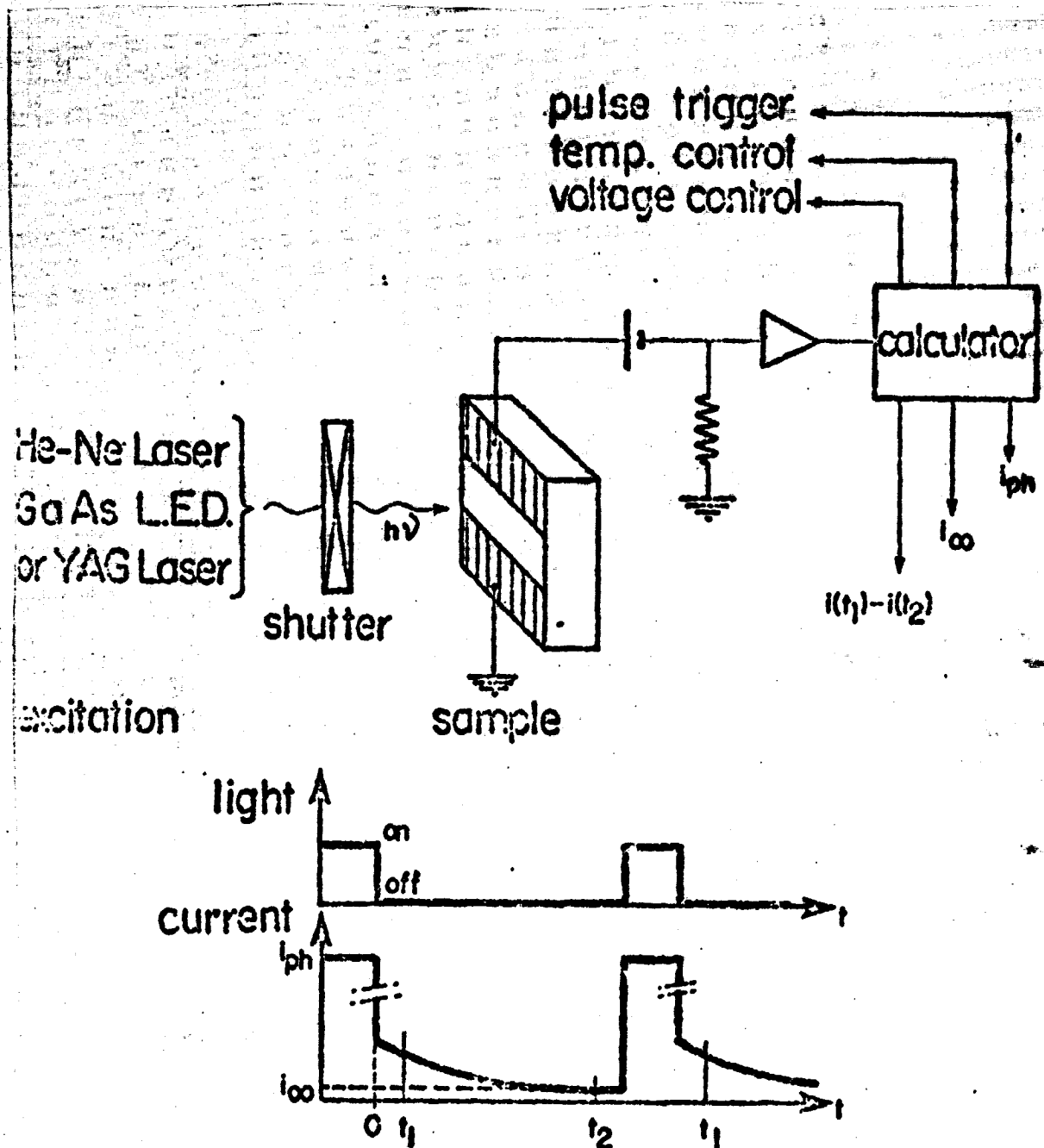


Fig : 1

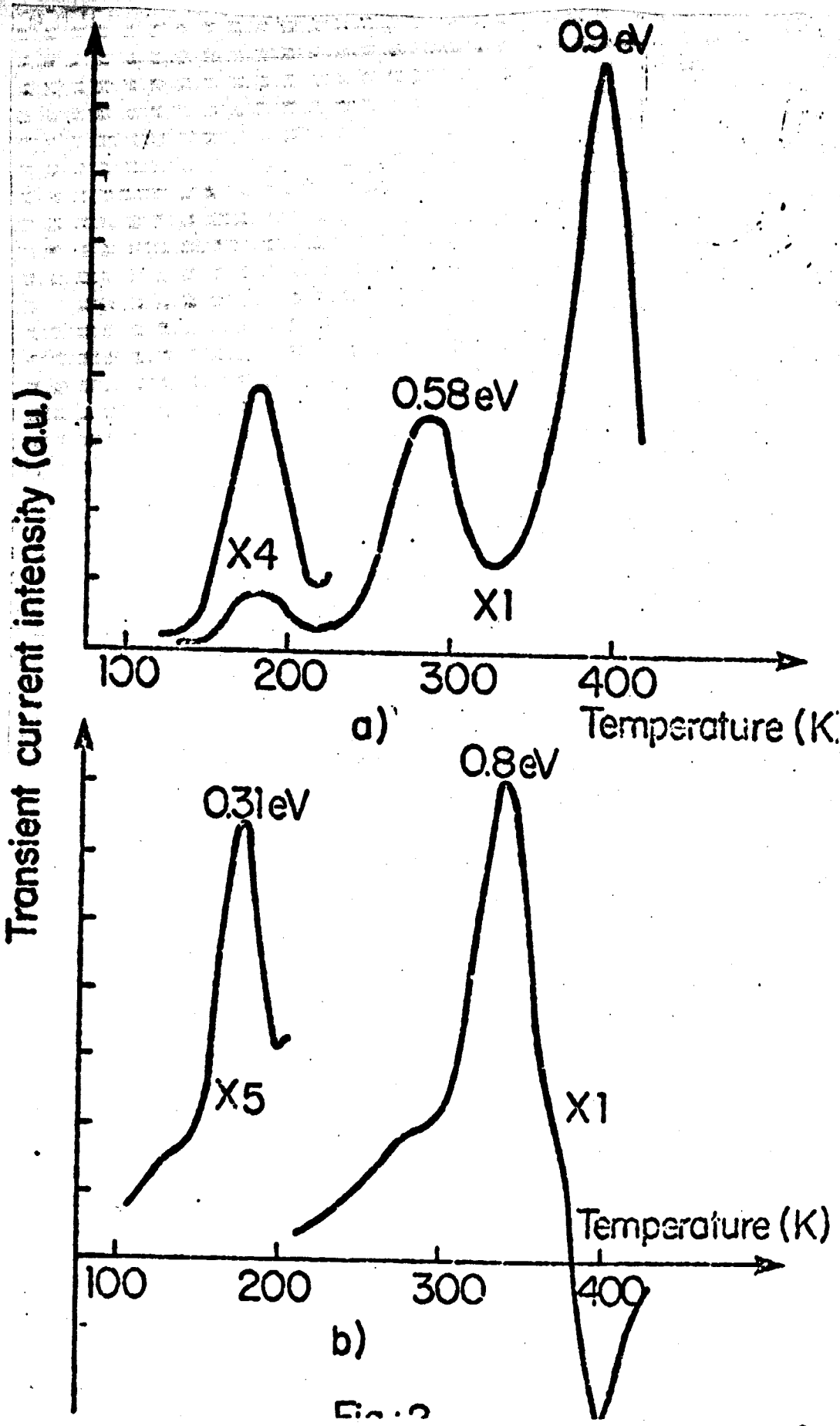


Fig. 2

ORIGINAL PAGE IS  
OF POOR QUALITY

